Dextramer$^+$ CTLs (99.9%) which did not react with HIV Dextramer (Fig. 2c). These results indicate that $GPC3_{144–152}$ peptide-specific CTL clones were successfully established from PBMCs of patients injected with $GPC3_{144–152}$ peptide vaccine by three different methods. Moreover, the result that patient A2-8 CTL clone that reacted to HepG2 had $GPC3_{144–152}$ peptide specificity verified that $GPC3_{144–152}$ peptide was present naturally on HepG2.

Analysis of $GPC3_{144–152}$ peptide-specific avidity of three CTL clones. To further characterize the $GPC3_{144–152}$ peptide-specific avidity of the three CTL clones, we tested for the lysis of T2 cells pulsed with decreasing concentrations of $GPC3_{144–152}$ or $HIV_{19–27}$ peptide ranging from 10^{-6} to 10^{-14} M. The peptide concentration at which the curve crossed 50% cytotoxicity was defined as the recognition efficiency of that clone. The recognition efficiencies of patient A2-9, A2-14, and A2-8 clones were 10^{-10}, 10^{-10}, and 10^{-11} M, respectively (Fig. 3). These CTL clones did not react against T2 cells pulsed with $HIV_{19–27}$ peptide. These results indicate that the established clones were $GPC3_{144–152}$ peptide-specific and high avidity CTLs.

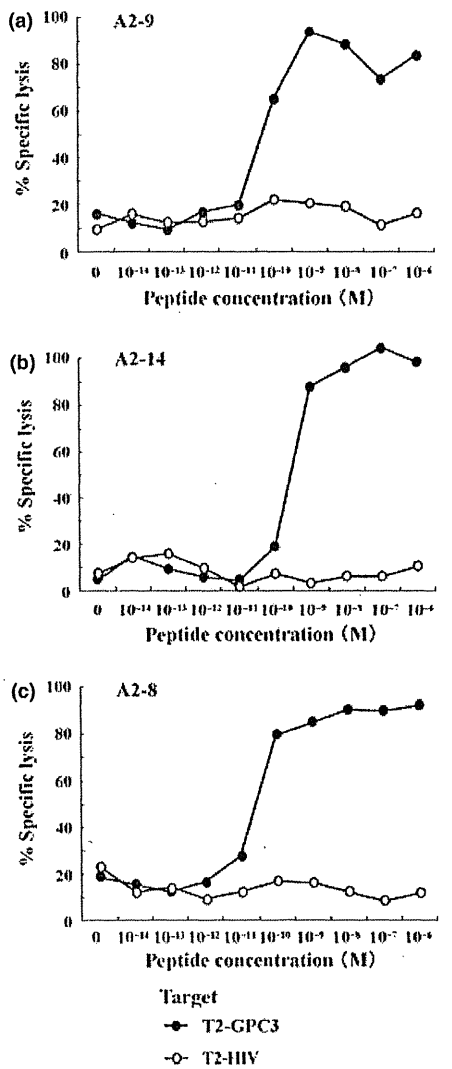

Fig. 3. Analysis of the $GPC3_{144–152}$ peptide specific avidity of the three CTL clones. The established CTL clones were tested for their avidities using various concentrations of $GPC3_{144–152}$ (●) or $HIV_{19–27}$ (○) peptide-loaded T2 targets. The peptide concentration at which the curve crossed 50% cytotoxicity was defined as the recognition efficiency of that clone. Effector/target ratio = 10. The recognition efficiencies of patient A2-9 (a), A2-14 (b), and A2-8 (c) CTL clones were 10^{-10}, 10^{-10}, and 10^{-11} M, respectively.

Reactivity of three CTL clones against cancer cell lines. We analyzed the IFN-γ production and cytotoxicity of the established CTL clones against cancer cell lines expressing HLA-A*02:01 and GPC3. We used SK-Hep-1 (GPC3$^-$, HLA-A*02:01$^+$) and a human GPC3 gene transfectant, SK-Hep-1/hGPC3 (GPC3$^+$, HLA-A*02:01$^+$), as target cells. Production of IFN-γ in the three CTL clones was detected against SK-Hep-1/hGPC3, but not against SK-Hep-1 (Fig. 4a). Furthermore, these CTL clones showed specific cytotoxicity against SK-Hep-1/hGPC3 and HepG2 (GPC3$^+$, HLA-A*02:01$^+$), but not against SK-Hep-1 and SW620 (GPC3$^-$, HLA-A*02:01$^+$) (Fig. 4b). These results indicate that all three CTL clones show cytotoxicity and the ability to produce IFN-γ against HLA-A*02:01$^+$ GPC3$^+$ HCC cell lines. Next, we examined whether these CTL clones respond to cancer cells weakly expressing GPC3. We used human melanoma cell line 526mel (GPC3$^+$, HLA-A*02:01$^+$) as a target cell that expresses GPC3 mRNA and protein at a lower level than the HCC cell lines (data not shown). Production of IFN-γ in patient A2-8 CTL clone (recognition efficiency: 10^{-11} M) were clearly detected against 526mel, whereas patient A2-9 CTL clone (recognition efficiency: 10^{-10} M) showed weak response to 526mel (Fig. 4c). Similarly, patient A2-8 CTL clone showed specific cytotoxicity against 526mel, whereas patient A2-9 CTL clone failed to lyse 526mel (Fig. 4d). These results suggest that higher avidity is essential to react to cancer cells weakly expressing GPC3.

Analysis of HLA-A2 and GPC3 restriction. In a cold target inhibition assay, cytotoxicity against SK-Hep-1/hGPC3 of patient A2-9 clone was suppressed by the addition of $GPC3_{144–152}$ peptide-pulsed T2 cells but not by the addition of $HIV_{19–27}$ peptide-pulsed T2 cells (Fig. 5a). In an HLA blocking experiment, the IFN-γ production of patient A2-9 CTL clone was markedly inhibited by anti-HLA class I mAb and anti-HLA-A2 mAb as compared with that by IgG2a or IgG2b isotype control ($P < 0.05$) (Fig. 5b). Similarly, the cytotoxicity against SK-Hep-1/hGPC3 of patient A2-9 clone was markedly inhibited by anti-HLA class I mAb and anti-HLA-A2 mAb compared with that by IgG2a and IgG2b isotype control ($P < 0.05$) (Fig. 5c). These results clearly indicate that the CTL clone recognized SK-Hep-1/hGPC3 in an HLA-A2-restricted manner.

Next, to ascertain the GPC3 antigen-specific response of a CTL clone, we examined GPC3 knockdown using siRNA on the GPC3$^+$ HepG2 cell line. Representative data are shown in Figure 5(d–f). The GPC3 expression of HepG2 was clearly decreased by GPC3 siRNA on RT-PCR (Fig. 5d). Specifically, the GPC3 expression of HepG2 was decreased from 24 to 72 h following treatment with GPC3 siRNA on Western blot (Fig. 5e). We examined the IFN-γ production of patient A2-9 CTL clone against HepG2 treated with GPC3 siRNA. The IFN-γ production of the CTL clone was significantly decreased by GPC3 siRNA ($P < 0.05$) (Fig. 5f). These results indicate that HLA-A2-restricted $GPC3_{144–152}$ peptide can be processed naturally by cancer cells, and the peptides in the context of HLA-A2 can be expressed on the cell surface of cancer cells in order to be recognized by a $GPC3_{144–152}$ peptide-specific CTL clone.

Discussion

Salgaller *et al.*[17] failed to detect dose dependency between 1 and 10 mg in terms of the capacity of gp100 peptide to enhance immunogenicity in humans. Previously, we reported that the peptide emulsified with incomplete Freund's adjuvant is stable, although the peptide is easily degraded in serum.[16] In this study, as with our previous report using a mouse model,[16] we

doi: 10.1111/j.1349-7006.2011.01896.x

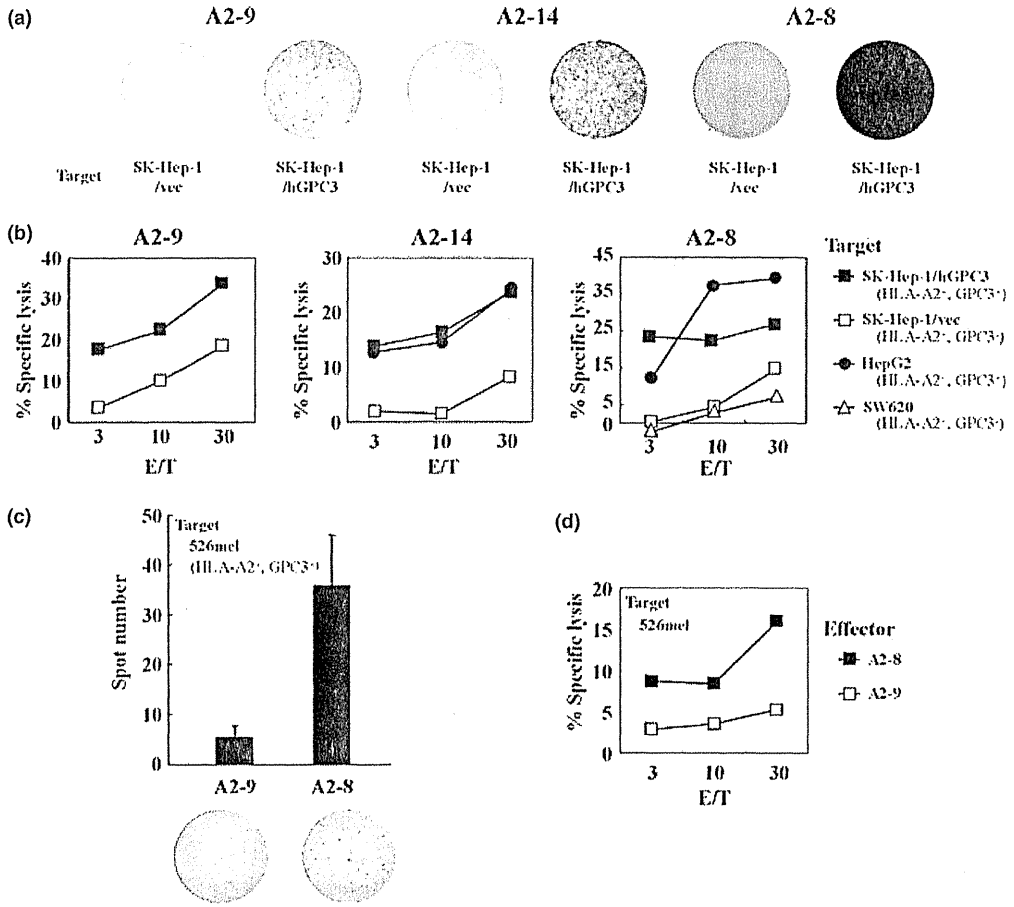

Fig. 4. Reactivity of three CTL clones against cancer cell lines. (a) γ-Interferon enzyme-linked immunospot assay of established CTL clones against SK-Hep-1/hGPC3 and SK-Hep-1/vec. Effector/target (E/T) ratio = 0.2. (b) Cytotoxic activities of the three CTL clones against SK-Hep-1/hGPC3 (■), SK-Hep-1/vec (□), HepG2 (●), or SW620 (Δ) analyzed by cytotoxicity assay. (c) γ-Interferon enzyme-linked immunospot assay of established CTL clones against 526mel. E/T ratio = 0.2. (d) Cytotoxic activities of patient A2-8 (■) and A2-9 (□) CTL clone against 526mel analyzed by cytotoxicity assay.

found that the effect of $GPC3_{144–152}$ peptide emulsified with incomplete Freund's adjuvant between 0.3 and 30 mg, to induce specific CTLs, was dose-dependent.

$GPC3_{144–152}$ (FVGEFFTDV) peptide was previously identified as an HLA-A*02:01-restricted peptide.[15] Moreover, we confirmed by binding assay that the peptide could also bind HLA-A*02:06 and HLA-A*02:07 molecules (data not shown). Therefore, we carried out a clinical trial for three types of HLA-A2 patient. Indeed, similar to HLA-A*02:01 patients, $GPC3_{144–152}$ peptide-specific CTLs increased after vaccination in both HLA-A*02:06 and HLA-A*02:07 patients (Fig. 1b). These findings suggest that $GPC3_{144–152}$ peptide is useful for not only HLA-A*02:01 patients but also HLA-A*02:06 and HLA-A*02:07 patients.

Notably, previous reports have shown that vaccination with synthetic peptides occassionally induced ineffective CTL responses due to various underlying mechanisms.[4–9] A possible mechanism is that responding T cells may have a very low affinity such that they recognize only target cells pulsed with high concentrations of the peptide and not tumor cells expressing the relevant epitopes at lower copy numbers. Alternatively, some antigen epitopes were not expressed on the surface of tumor cells.[18,19] When evaluating T-cell response to peptide vaccines, it is important to confirm that responding CTLs lyse human cancer cells. In the present study, although CTL clones established by Dextramer assay could react to HLA-A*02:01$^+$ GPC3$^+$ HCC cell lines, these clones failed to react to the HLA-A*02:01$^+$ GPC3$^+$ melanoma cell line 526mel expressing GPC3 mRNA and protein at a lower level than the HCC cell lines. Therefore, we attempted to establish CTL clones that are more tumor-reactive and with higher avidity than CTL clones established by Dextramer assay. Rubio *et al.*[20] showed that the surface mobilization of CD107a was useful for identifying and isolating functional tumor-reactive T cells with high recognition efficiency directly from PBMCs of cancer patients after vaccination. In the present study, the CTL clone showing the highest avidity (10^{-11} M) and tumor reactivity was established by CD107a mobilization assay. Moreover, this clone could also react to 526mel.

For patients with metastatic melanoma, adoptive cell therapy has emerged as the most effective treatment.[21,22] However, tumor-infiltrating lymphocytes with high avidity for tumor antigens can only be generated from some patients with melanoma.[21] Recent studies have shown that genes encoding T-cell receptors (TCRs) can be isolated from high avidity T cells that recognize cancer antigens, and retroviral or lentiviral vectors can be used to redirect lymphocyte specificity to these cancer antigens.[23–26] In the present study, we were able to successfully establish some high avidity CTL clones. We analyzed the TCR β-chain variable region gene families of these clones by

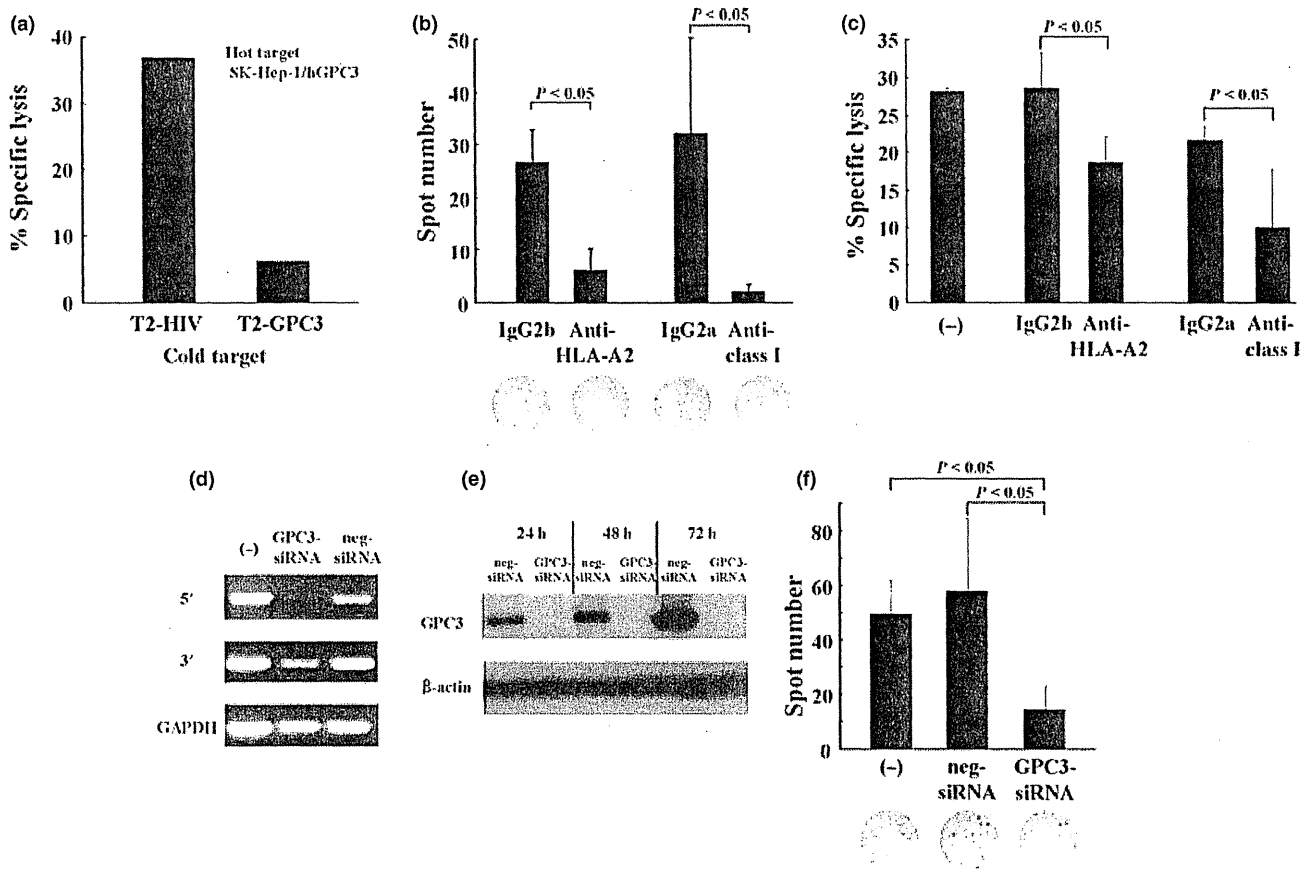

Fig. 5. Analysis of HLA-A2 and glypican-3 (GPC3) restriction. (a) Cold target inhibition assay of patient A2-9 CTL clone against SK-Hep-1/hGPC3. Effector/target (E/T) ratio = 30. T2 was prepulsed with either HIV_{19-27} peptide or $GPC3_{144-152}$ peptide, then used as cold target cells. Cold/hot target ratio = 10. The cytotoxicity of the CTL clone was inhibited by T2 pulsed with $GPC3_{144-152}$ peptide but not by T2 pulsed with HIV_{19-27} peptide. (b) Inhibition of interferon (IFN)-γ production by anti-HLA class I mAb and anti-HLA A2 mAb. SK-Hep-1/hGPC3 used as target cells. E/T ratio = 0.02. The IFN-γ production of the CTL clone was markedly inhibited by anti-HLA class I mAb and anti-HLA-A2 mAb as compared with that by IgG2a and IgG2b isotype control ($P < 0.05$). Data are expressed as the mean ± SD. (c) Inhibition of cytotoxicity by anti-HLA class I mAb and anti-HLA A2 mAb. SK-Hep-1/hGPC3 used as target cells. E/T ratio = 30. The cytotoxicity of the CTL clone was markedly inhibited by anti-HLA class I mAb and anti-HLA-A2 mAb compared with that by IgG2a and IgG2b isotype control ($P < 0.05$). (d) The GPC3 expression on HepG2 treated with GPC3-siRNA or negative (neg)-siRNA for 24 h as determined by RT-PCR. (e) The GPC3 expression on HepG2 treated with GPC3-siRNA or neg-siRNA from 24 to 72 h as determined by Western blot analysis. The GPC3 expression of HepG2 was decreased from 24 to 72 h after treatment with GPC3 siRNA. (f) The IFN-γ production of the CTL clone against HepG2 treated with GPC3 siRNA. E/T ratio = 0.02. The IFN-γ production of the CTL clone was decreased by GPC3 siRNA ($P < 0.05$). Data are expressed as the mean ± SD.

RT-PCR and carried out gene sequencing (data not shown). These clones had different TCR genes. Our results raise the possibility that these clones might be applicable to adoptive cell therapy for a large number of HCC patients.

In conclusion, we proved in this study the dose-dependent effects of highly immunogenic $GPC3_{144-152}$ peptide. Furthermore, we provided substantial evidence that CTLs showing not only high avidity but also natural antigen-specific killing activity against HCC cells could be induced in HCC patients by peptide vaccine.

Acknowledgments

This work was supported in part by Grants-in-Aid for Research on Hepatitis and for Clinical Research from the Ministry of Health, Labour and Welfare, Japan, and a Research Grant of the Princess Takamatsu Cancer Research Fund.

Disclosure Statement

The authors have no conflict of interest.

References

1 Rosenberg SA, Yang JC, Schwartzentruber DJ *et al.* Immunologic and therapeutic evaluation of a synthetic peptide vaccine for the treatment of patients with metastatic melanoma. *Nat Med* 1998; 4: 321–7.
2 Thurner B, Haendle I, Roder C *et al.* Vaccination with mage-3A1 peptide-pulsed mature, monocyte-derived dendritic cells expands specific cytotoxic T cells and induces regression of some metastases in advanced stage IV melanoma. *J Exp Med* 1999; **190**: 1669–78.
3 Marchand M, van Baren N, Weynants P *et al.* Tumor regressions observed in patients with metastatic melanoma treated with an antigenic peptide encoded by gene MAGE-3 and presented by HLA-A1. *Int J Cancer* 1999; **80**: 219–30.
4 Yamshchikov GV, Barnd DL, Eastham S *et al.* Evaluation of peptide vaccine immunogenicity in draining lymph nodes and peripheral blood of melanoma patients. *Int J Cancer* 2001; **92**: 703–11.
5 Matsui M, Moots RJ, Warburton RJ *et al.* Genetic evidence for difference between intracellular and extracellular peptides in influenza A matrix peptide-specific CTL recognition. *J Immunol* 1995; **154**: 1088–96.

doi: 10.1111/j.1349-7006.2011.01896.x

6 Falo LD Jr, Colarusso LJ, Benacerraf B *et al.* Serum proteases alter the antigenicity of peptides presented by class I major histocompatibility complex molecules. *Proc Natl Acad Sci USA* 1992; **89**: 8347–50.
7 Amoscato AA, Prenovitz DA, Lotze MT. Rapid extracellular degradation of synthetic class I peptides by human dendritic cells. *J Immunol* 1998; **161**: 4023–32.
8 Chen W, Yewdell JW, Levine RL *et al.* Modification of cysteine residues in vitro and in vivo affects the immunogenicity and antigenicity of major histocompatibility complex class I-restricted viral determinants. *J Exp Med* 1999; **189**: 1757–64.
9 Meadows L, Wang W, den Haan JM *et al.* The HLA-A*0201-restricted H-Y antigen contains a posttranslationally modified cysteine that significantly affects T cell recognition. *Immunity* 1997; **6**: 273–81.
10 Nakatsura T, Yoshitake Y, Senju S *et al.* Glypican-3, overexpressed specifically in human hepatocellular carcinoma, is a novel tumor marker. *Biochem Biophys Res Commun* 2003; **306**: 16–25.
11 Shirakawa H, Suzuki H, Shimomura M *et al.* Glypican-3 expression is correlated with poor prognosis in hepatocellular carcinoma. *Cancer Sci* 2009; **100**: 1403–7.
12 Nakatsura T, Komori H, Kubo T *et al.* Mouse homologue of a novel human oncofetal antigen, glypican-3, evokes T-cell-mediated tumor rejection without autoimmune reactions in mice. *Clin Cancer Res* 2004; **10**: 8630–40.
13 Nakatsura T, Kageshita T, Ito S *et al.* Identification of glypican-3 as a novel tumor marker for melanoma. *Clin Cancer Res* 2004; **10**: 6612–21.
14 Motomura Y, Senju S, Nakatsura T *et al.* Embryonic stem cell-derived dendritic cells expressing glypican-3, a recently identified oncofetal antigen, induce protective immunity against highly metastatic mouse melanoma, B16-F10. *Cancer Res* 2006; **66**: 2414–22.
15 Komori H, Nakatsura T, Senju S *et al.* Identification of HLA-A2- or HLA-A24-restricted CTL epitopes possibly useful for glypican-3-specific immunotherapy of hepatocellular carcinoma. *Clin Cancer Res* 2006; **12**: 2689–97.
16 Motomura Y, Ikuta Y, Kuronuma T *et al.* HLA-A2 and -A24-restricted glypican-3-derived peptide vaccine induces specific CTLs: preclinical study using mice. *Int J Oncol* 2008; **32**: 985–90.
17 Salgaller ML, Marincola FM, Cormier JN *et al.* Immunization against epitopes in the human melanoma antigen gp100 following patient immunization with synthetic peptides. *Cancer Res* 1996; **56**: 4749–57.
18 So T, Hanagiri T, Chapiro J *et al.* Lack of tumor recognition by cytolytic T lymphocyte clones recognizing peptide 195–203 encoded by gene MAGE-A3 and presented by HLA-A24 molecules. *Cancer Immunol Immunother* 2007; **56**: 259–69.
19 Sorensen RB, Junker N, Kirkin A *et al.* The immunodominant HLA-A2-restricted MART-1 epitope is not presented on the surface of many melanoma cell lines. *Cancer Immunol Immunother* 2009; **58**: 665–75.
20 Rubio V, Stuge TB, Singh N *et al.* Ex vivo identification, isolation and analysis of tumor-cytolytic T cells. *Nat Med* 2003; **9**: 1377–82.
21 Rosenberg SA, Restifo NP, Yang JC *et al.* Adoptive cell transfer: a clinical path to effective cancer immunotherapy. *Nat Rev Cancer* 2008; **8**: 299–308.
22 Dudley ME, Yang JC, Sherry R *et al.* Adoptive cell therapy for patients with metastatic melanoma: evaluation of intensive myeloablative chemoradiation preparative regimens. *J Clin Oncol* 2008; **26**: 5233–9.
23 Morgan RA, Dudley ME, Wunderlich JR *et al.* Cancer regression in patients after transfer of genetically engineered lymphocytes. *Science* 2006; **314**: 126–9.
24 Cole DJ, Weil DP, Shilyansky J *et al.* Characterization of the functional specificity of a cloned T-cell receptor heterodimer recognizing the MART-1 melanoma antigen. *Cancer Res* 1995; **55**: 748–52.
25 Hughes MS, Yu YY, Dudley ME *et al.* Transfer of a TCR gene derived from a patient with a marked antitumor response conveys highly active T-cell effector functions. *Hum Gene Ther* 2005; **16**: 457–72.
26 Morgan RA, Dudley ME, Yu YY *et al.* High efficiency TCR gene transfer into primary human lymphocytes affords avid recognition of melanoma tumor antigen glycoprotein 100 and does not alter the recognition of autologous melanoma antigens. *J Immunol* 2003; **171**: 3287–95.

Radiofrequency ablation for hepatocellular carcinoma induces glypican-3 peptide-specific cytotoxic T lymphocytes

DAISUKE NOBUOKA[1,4*], YUTAKA MOTOMURA[1,5*], HIROFUMI SHIRAKAWA[1], TOSHIAKI YOSHIKAWA[1], TOSHIMITSU KURONUMA[1], MARI TAKAHASHI[1], KOHEI NAKACHI[2], HIROSHI ISHII[2], JUNJI FURUSE[2], NAOTO GOTOHDA[3], SHINICHIRO TAKAHASHI[3], TOSHIO NAKAGOHRI[3], MASARU KONISHI[3], TAIRA KINOSHITA[3], HIROYUKI KOMORI[5], HIDEO BABA[5], TOSHIYOSHI FUJIWARA[4] and TETSUYA NAKATSURA[1]

[1]Section for Cancer Immunotherapy, Investigative Treatment Division, Research Center for Innovative Oncology, [2]Division of Hepatobiliary and Pancreatic Oncology, [3]Division of Digestive Surgery, National Cancer Center Hospital East, 6-5-1 Kashiwanoha, Kashiwa, Chiba 277-8577; [4]Department of Gastroenterological Surgery, Okayama University Graduate School of Medicine, Dentistry, and Pharmaceutical Sciences, 2-5-1 Shikata-cho, Okayama 700-8558; [5]Department of Gastroenterology and Hepatology, Graduate School of Medical Sciences, Kumamoto University, 1-1-1 Honjo, Kumamoto 860-8556, Japan

Received July 9, 2011; Accepted August 25, 2011

DOI: 10.3892/ijo.2011.1202

Abstract. Glypican-3 (GPC3), a carcinoembryonic antigen, is an ideal target for anticancer immunotherapy against hepatocellular carcinoma (HCC). In this study, we attempted to compare the induction of the GPC3-specific T-cell-mediated immune response after locoregional therapies in HCC patients and tumor-bearing mice. Twenty-seven HCC patients treated with locoregional therapies, including radiofrequency ablation (RFA), surgical resection and transcatheter arterial chemoembolization (TACE), were prospectively enrolled in this study. Additionally, we performed RFA experiments using a mouse model. GPC3-specific T-cell response was investigated pre-treatment and post-treatment by an interferon-γ enzyme-linked immunospot assay using peripheral blood mononuclear cells from HCC patients and lymph node cells from tumor-bearing mice. Circulating GPC3-specific cytotoxic T lymphocytes (CTLs) were increased in 5 of 9 patients after RFA and in 4 of 9 patients after TACE, but in only 1 of 9 patients after surgical resection. All 7 patients with GPC3-expressing HCCs exhibited an increase in GPC3-specific CTLs after RFA or TACE, whereas none of the 7 patients did after surgical resection. The number of increased GPC3-specific CTLs after RFA was significantly larger than that after surgical resection (P=0.023). Similarly, the frequency of GPC3-specific CTLs after RFA was significantly greater than that after surgical resection in the mouse model (P=0.049). We validated for the first time the stronger effect on the immune system brought by RFA compared with surgical resection for HCC patients and tumor-bearing mice. Combined treatment of RFA and immunotherapy is a reasonable strategy against HCC.

Correspondence to: Dr Tetsuya Nakatsura, Section for Cancer Immunotherapy, Investigative Treatment Division, Research Center for Innovative Oncology, National Cancer Center Hospital East, 6-5-1 Kashiwanoha, Kashiwa, Chiba 277-8577, Japan
E-mail: tnakatsu@east.ncc.go.jp

*Contributed equally

Abbreviations: GPC3, glypican-3; HCC, hepatocellular carcinoma; RFA, radiofrequency ablation; TACE, transcatheter arterial chemoembolization; CTL, cytotoxic T lymphocyte; CT, computed tomography; TNM, tumor-node-metastasis; UICC, the Union for International Cancer Control; PBMC, peripheral blood mononuclear cell; IFN, interferon; ELISPOT, enzyme-linked immunospot; HSP105, heat shock protein 105; CMV, cytomegalovirus; AFP, α-fetoprotein; PIVKA-II, protein induced by vitamin K absence or antagonist II; hTERT, human telomerase reverse transcriptase; MRP3, multidrug resistance-associated protein 3

Key words: hepatocellular carcinoma, radiofrequency ablation, glypican-3, cytotoxic T lymphocyte, immunotherapy

Introduction

Hepatocellular carcinoma (HCC) is one of the most common and most serious cancers worldwide (1). Locoregional therapies, including radiofrequency ablation (RFA), surgical resection, and transcatheter arterial chemoembolization (TACE), are recognized as the gold-standard therapies for HCC patients whose cancer lesions are limited to the liver (2). However, the recurrence rate remains quite high despite potentially curative treatment (3,4). The reasons for this are as follows: first, a multicentric new tumor frequently occurs from underlying active hepatitis or cirrhosis and, second, a small tumor undetectable by imaging modalities frequently exists before treatment and would be left untreated (5). Therefore, the establishment of effective adjuvant therapy to prevent recurrence is urgently required, and

clinical trials are ongoing throughout the world (6). However, at the present time, there is no universal consensus (2,7,8).

Previous studies have reported that local tumor ablation treatments, such as RFA and cryoablation, not only destroy tumor tissue but also induce a marked inflammatory response both locally and systemically (9,10). Unlike surgical resection, tumor ablation treatment generates tumor cell necrosis (11), followed by the release of tumor-associated antigens (12). These antigens can be uptaken, processed, and presented by dendritic cells (10,13), and then an antigen-specific T-cell-mediated immune response can be induced (9). If this induction is sufficiently steady and reliable, it may provide the basis for adjuvant immunotherapy, which is an attractive strategy.

Glypican-3 (GPC3) belongs to the glypican family of heparan sulfate proteoglycans that are linked to the outer surface of the cell membrane through a glycosylphosphatidylinositol anchor (14). GPC3 is one of the carcinoembryonic antigens overexpressed in HCC (15-17). We have shown that GPC3 is an ideal target for anticancer immunotherapy because its expression is specifically detected in ~80% of HCCs even in the early stages and is correlated with a poor prognosis (18-21). Moreover, GPC3-specific cytotoxic T lymphocytes (CTLs) have a high level of killing activity against HCC tumor cells (22). We have finished the phase I clinical trial of a GPC3-derived peptide vaccine for patients with advanced HCC (unpublished data), and just started the phase II clinical trial for adjuvant therapy after curative resection or RFA.

In this study, our aim was to determine if the GPC3-specific T-cell-mediated immune response is strengthened after locoregional therapies in HCC patients and tumor-bearing mice. Moreover, we evaluated the hypothesis that the post-treatment immune response may provide the basis for adjuvant immunotherapy.

Materials and methods

Patient population and treatment of HCC. Twenty-seven patients with primary HCC were prospectively enrolled in this study from January to November 2007 at the National Cancer Center Hospital East, in Japan. The eligibility criteria included primary HCC, which would undergo locoregional therapies with curative intent. Three treatment groups of nine patients each would undergo RFA, surgical resection, or TACE, respectively. Treatment selection in each patient was in accordance with the Japanese HCC treatment guidelines (2). Other inclusion criteria included HLA-A24 or HLA-A2 gene-positive status, as determined by commercially-available genomic DNA typing tests (Mitsubishi Chemical Medience, Tokyo, Japan), and no other active malignancy. HCC was diagnosed using dynamic computed tomography (CT). Tumor stage was assigned according to the tumor-node-metastasis (TNM) classification of the Union for International Cancer Control (UICC) (23). All RFA procedures were performed percutaneously under ultrasound guidance. Curative treatment was defined as complete necrosis of the tumor lesion confirmed by dynamic CT after RFA, a negative surgical margin confirmed histopathologically after resection, and complete lipiodol deposition after TACE.

All patients gave written informed consent before entering the study and this study was approved by the Ethics Committee of the National Cancer Center, conforming to the ethical guidelines of the 1975 Declaration of Helsinki.

Collection of blood samples and preparation of peripheral blood mononuclear cells. Venous blood (20-30 ml) from each patient was collected both before treatment and one month after treatment. Peripheral blood mononuclear cells (PBMCs) were separated from whole blood using LeucoSep® tubes (Greiner Bio-One, Frickenhausen, Germany) by means of density gradient centrifugation.

Identification of GPC3-specific CTLs in HCC patients. In order to identify GPC3-specific CTLs, the proportion of cells producing interferon (IFN)-γ upon stimulation with GPC3 peptide was assessed by an *ex vivo* IFN-γ enzyme-linked immunospot (ELISPOT) assay using pooled PBMCs from HCC patients. Defrosted PBMCs ($1x10^6$ cells/well) were cultured in duplicate using 96-well flat-bottomed plates (BD Biosciences, San Jose, CA) with HLA-A24-restricted $GPC3_{298-306}$ peptide (EYILSLEEL) or HLA-A2-restricted $GPC3_{144-152}$ peptide (FVGEFFTDV) (10 μmol/l) with 100 U/ml recombinant human interleukin-2 (IL-2) for 20 h. The negative control consisted of medium alone or HLA-A24- or HLA-A2-restricted heat shock protein 105 (HSP105) peptide, and the positive control included the HLA-A24- or HLA-A2-restricted cytomegalovirus (CMV) peptide. The number of spots, which indicated the presence of IFN-γ secreting cells, was automatically counted using the Eliphoto system (Minerva Tech, Tokyo, Japan). For an exact comparison of the frequency of GPC3-specific CTLs existing at pre- and post-treatment, the obtained mean values of the number of spots with non-peptide-pulsed samples ($1x10^6$ PBMCs) at pre- and post-treatment were equalized and set to zero, and then the actual number of GPC3-, CMV-, or HSP105-specific spots was calculated. The Δspot was defined as the difference in the number of spots with each antigen between pre- and post-treatment.

Mice. Female BALB/c mice ($H\text{-}2^d$), 6-8 weeks of age, were obtained from Charles River Laboratories Japan (Yokohama, Japan). The mice were maintained under specific-pathogen-free conditions. All animal procedures were performed in compliance with the guidelines by the Animal Research Committee of the National Cancer Center, Japan.

Tumor cell lines. A subline of the BALB/c-derived GPC3-negative colorectal adenocarcinoma cell line, Colon 26 (24), was provided by Dr Kyoichi Shimomura (Astellas Pharma, Tokyo, Japan). Colon 26/GPC3 is an established stable GPC3-expressing cell line (18). The cells were cultured in RPMI-1640 medium supplemented with 10% fetal bovine serum, 100 U/ml penicillin, and 100 μg/ml streptomycin in humidified 5% CO_2 at 37˚C.

RFA experiment using a mouse model. The mice were shaved at the tumor area and the contralateral flank. After attachment of the electricity-conducting pad (ground pad) onto the contralateral side, an RFA needle with 5-mm active tip (Cool-tip™, Valleylab, Boulder, CO) was inserted into the middle of the tumor. Impedance could be evaluated on the RFA lesion generator system (RFG-3B model, Radionics, Burlington, MA).

Treatment was started by delivering RFA energy. During two treatment cycles of 10 sec, the temperature could be monitored using the thermistor and thermocouple in the tip of the probe. Treatment was considered successful if a tip temperature of 60-70°C was reached.

Identification of GPC3-specific CTLs in mice. BALB/c mice were immunized beforehand by peptide vaccination with K^d-restricted $GPC3_{298-306}$ peptide (50 μg/mouse) emulsified with incomplete Freund's adjuvant twice at a 7-day interval as described previously (20). The day after the second vaccination, the mice were challenged subcutaneously with Colon 26/GPC3 tumor cells ($1x10^5$ cells/100 μl) on their shaved back and, 5 days later, the mice underwent therapeutic RFA or surgical resection for the established tumor. After the next 5 days, the mice were sacrificed and bilateral inguinal lymph nodes were obtained. $CD8^+$ T cells were isolated from lymph node cells using anti-mouse CD8α (Ly-2) microbeads (Miltenyi Biotec, Bergisch Gladbach, Germany) and an IFN-γ ELISPOT assay was performed without prior *in vitro* stimulation. For the IFN-γ ELISPOT assay, $CD8^+$ lymph node cells ($3x10^5$ cells/well) were used as effector cells, and Colon 26 and Colon 26/GPC3 cells ($3x10^4$ cells/well) as target cells. These cells were cultured in duplicate using 96-well flat-bottomed plates (BD Biosciences) with 100 U/ml recombinant murine IL-2 for 20 h. The number of spots after RFA or surgical resection was compared with that without treatment.

Immunohistochemical analysis. To investigate GPC3 expression in HCC tissues, we performed immunohistochemical staining of GPC3 in biopsy specimens or resected specimens from HCC patients. The paraffin-embedded blocks were analyzed using monoclonal anti-GPC3 antibody (dilution 1:300, BioMosaics, Burlington, VT) as described previously (17,21). The results were classified into two groups according to the area of GPC3-positive staining cells as follows: -, negative (<10%) and +, positive (≥10%).

To investigate tumor-infiltrating lymphocytes, we performed immunohistochemical staining of CD4 and CD8 in resected specimens from an HCC patient using monoclonal anti-CD4 or CD8 antibody (dilution 1:20, Novocastra, Newcastle upon Tyne, UK).

Statistical analysis. Statistical analyses were performed using χ^2 test, Mann-Whitney U test, or Kruskal-Wallis rank test. Differences were considered significant at $P<0.05$. Data were analyzed with the StatView 5.0 software package (Abacus Concepts, Calabasas, CA).

Results

Demographics and clinical characteristics. The characteristics of all 27 patients are represented in Table I. The three groups of 9 patients received RFA (RFA1-9), surgical resection (RES1-9), or TACE (TAE1-9), respectively. Among them, 21 patients had the HLA-A24 gene and 7 had the HLA-A2 gene. One patient had both HLA-A24 and -A2, and the HLA-A2-restricted $GPC3_{144-152}$ peptide was used for the IFN-γ ELISPOT assay in this patient. Among the three treatment groups, tumor size in the RFA group (mean: 16.4 mm) was significantly smaller than that in the resection group (mean: 43.2 mm) (P=0.001) and the TACE group (mean: 44.1 mm) (P=0.001). Similarly, tumor stage in the RFA group was less advanced than that in the resection group (P=0.018) and TACE group (P=0.005). There was no statistically significant difference in Child-Pugh classification grade among the three groups (P=0.128). In this study, all treatments were considered to be curative according to the definitions described in Materials and methods. Moreover, all groups reduced the levels of α-fetoprotein (AFP) and protein induced by vitamin K absence or antagonist II (PIVKA-II) in most of HCC patients after treatment (data not shown). The diagnosis of HCC was histopathologically confirmed by biopsy specimens or resected specimens from 21 patients. GPC3 expression was detected by immunohistochemical staining in 14 of 21 patients.

Analysis of GPC3-specific CTLs in HCC patients. As shown in Table I, GPC3-specific CTLs were detected in 11 and 15 of 27 patients at pre- and post-treatment, respectively. In total, 19 patients had GPC3-specific CTLs at either pre- or post-treatment. There was no statistically significant correlation between the presence of GPC3-specific CTLs and clinical features, including HLA-A type (P=0.126), age (P=0.750), gender (P=0.764), HCV infection (P=0.674), HBV infection (P=0.764), Child-Pugh classification grade (P=0.404), tumor multiplicity (P=0.674), tumor size (P=0.650), HCC staging (P=0.155), serum AFP level (P=0.288), and serum PIVKA-II level (P=0.094). Among the 21 patients who had the information about GPC3 expression in their HCC tissue, patients with GPC3-expressing HCCs had GPC3-specific CTLs more frequently than those with GPC3-negative HCCs, but the difference was not statistically significant (P=0.053).

Changes in GPC3-specific CTLs between before and after treatment. In order to analyze the effect of anticancer treatment on GPC3-specific T-cell response, we compared the frequency of GPC3-specific CTLs in PBMCs before treatment with that after treatment. As shown in Table I and Fig. 1, an increase in GPC3-specific CTLs was found in 5 of 9 patients after RFA and in 4 of 9 after TACE, but in only 1 of 9 patients after resection. Of note, all of the 7 patients with GPC3-expressing HCCs exhibited an increase in GPC3-specific CTLs after RFA or TACE, whereas none of the 7 patients with GPC3-expressing HCCs did after surgical resection. The Δspot of GPC3 in the RFA group (mean: 24.4 spots) was larger than that in the resection group (mean: -7.2 spots) (P=0.023). The Δspot of GPC3 in the TACE group (mean, 36.9 spots) was also larger than that in the resection group, but the difference was not statistically significant (P=0.096). In contrast, the Δspot of CMV showed no difference among the three groups (P=0.498). Neither the existence of GPC3-specific CTLs before or after treatment, nor the changes between before and after treatment had statistically significant correlation with patient survival according to the log-rank test in each treatment group (neither disease-free nor overall), with the 27-month mean follow-up period (data not shown).

The representative data on changes in CT images and serum levels of tumor markers between before and after treatment is shown in Fig. 2. All three patients (RFA3, RES6, and TAE5) had GPC3-expressing HCCs. Both the CT images and

Table I. Patient characteristics and glypican-3-specific cytotoxic T lymphocytes.

Patient	HLA	Age (yrs.)	Gender	Etiology	Child-Pugh	No. of tumor	Tumor size (mm)	T[1]	N[1]	M[1]	AFP (<9.5 ng/ml)	PIVKA-II (<40 mAU/ml)	GPC3 expression[2]	GPC3-specific CTLs[3]			
														Pre	Post	Change	Δspot[4]
RFA1	A24	73	F	HBV	A	2	26	2	0	0	4.0	228	-	4	0	-	-4
RFA2	A24	68	M	HCV	B	1	20	1	0	0	5.0	300	+	10	24	+	+14
RFA3	A2	50	M	HCV	A	1	15	1	0	0	63.3	25	+	0	88	+	+88
RFA4	A24	79	F	HCV	A	1	10	1	0	0	484.2	30	+	0	10	+	+10
RFA5	A24	69	M	HCV	A	1	15	1	0	0	2.3	57	-	0	0	+/-	0
RFA6	A24	60	M	HCV	A	1	17	1	0	0	15.1	23	-	0	0	+/-	0
RFA7	A2	73	M	HCV	A	1	20	1	0	0	97.3	51	+	3	88	+	+85
RFA8	A2/A24	64	M	HBV/HCV	B	1	15	1	0	0	39.9	17	+	0	31	+	+31
RFA9	A2	60	M	HCV	B	1	10	1	0	0	92.0	19	-	19	15	-	-4
RES1	A24	48	M	HBV	A	1	20	1	0	0	19.7	38	+	32	15	-	-17
RES2	A24	66	F	HCV	A	1	26	2	0	0	63.4	77	+	20	3	-	-17
RES3	A24	64	M	HCV	A	2	30	2	0	0	10.1	276	+	12	0	-	-12
RES4	A2	72	M	-	A	1	60	2	0	0	9.2	1500	+	3	1	-	-2
RES5	A24	70	M	HCV	A	1	20	1	0	0	4.2	25	+	0	0	+/-	0
RES6	A24	42	M	HBV/HCV	A	2	98	3	0	0	15115.0	22477	+	50	30	-	-20
RES7	A2	75	M	-	A	1	75	2	0	0	22.8	10341	-	0	3	+	+3
RES8	A24	52	M	HCV	A	1	30	1	0	0	16.0	234	+	0	0	+/-	0
RES9	A24	60	M	HBV	A	1	30	1	0	0	15.6	23	-	0	0	+/-	0
TAE1	A2	64	M	-	A	3	30	2	0	0	10.7	98	+	0	330	+	+330
TAE2	A24	78	F	HCV	B	1	60	1	0	0	2483.0	3932	ND	34	0	-	-34
TAE3	A24	77	F	-	A	>5	35	3	0	0	180.2	11538	ND	0	3	+	+3
TAE4	A24	77	M	HCV	A	2	80	4	0	0	20014.0	241	ND	0	0	+/-	0
TAE5	A24	55	M	HBV	A	2	30	2	0	0	3.7	24	+	0	23	+	+23
TAE6	A24	77	M	-	A	>5	42	2	0	0	1407.0	1661	ND	0	20	+	+20
TAE7	A24	63	F	HCV	A	>5	32	2	0	0	640.3	270	ND	0	0	+/-	0
TAE8	A24	74	M	-	A	1	18	1	0	0	3.8	12	-	0	0	+/-	0
TAE9	A24	62	M	HCV	A	3	70	3	0	0	46.8	1907	ND	10	0	-	-10

[1]Tumor stage was assigned according to the tumor-node-metastasis (TNM) classification of the Union for International Cancer Control (UICC). [2]GPC3 expression was evaluated by immunohistochemical staining; +, positive; -, negative. [3]Peripheral blood was taken from each patient before and after treatment, and GPC3-specific CTLs were measured by *ex vivo* interferon-γ enzyme-linked immunospot assay; +, increase; -, decrease; +/-, no change. [4]The Δspot was defined as the difference in the number of spots with each antigen between pre- and post-treatment. F, female; M, male; HBV, hepatitis B virus; HCV, hepatitis C virus; AFP, α-fetoprotein; PIVKA-II, protein induced by vitamin K absence or antagonist II; GPC3, glypican-3; ND, not determined.

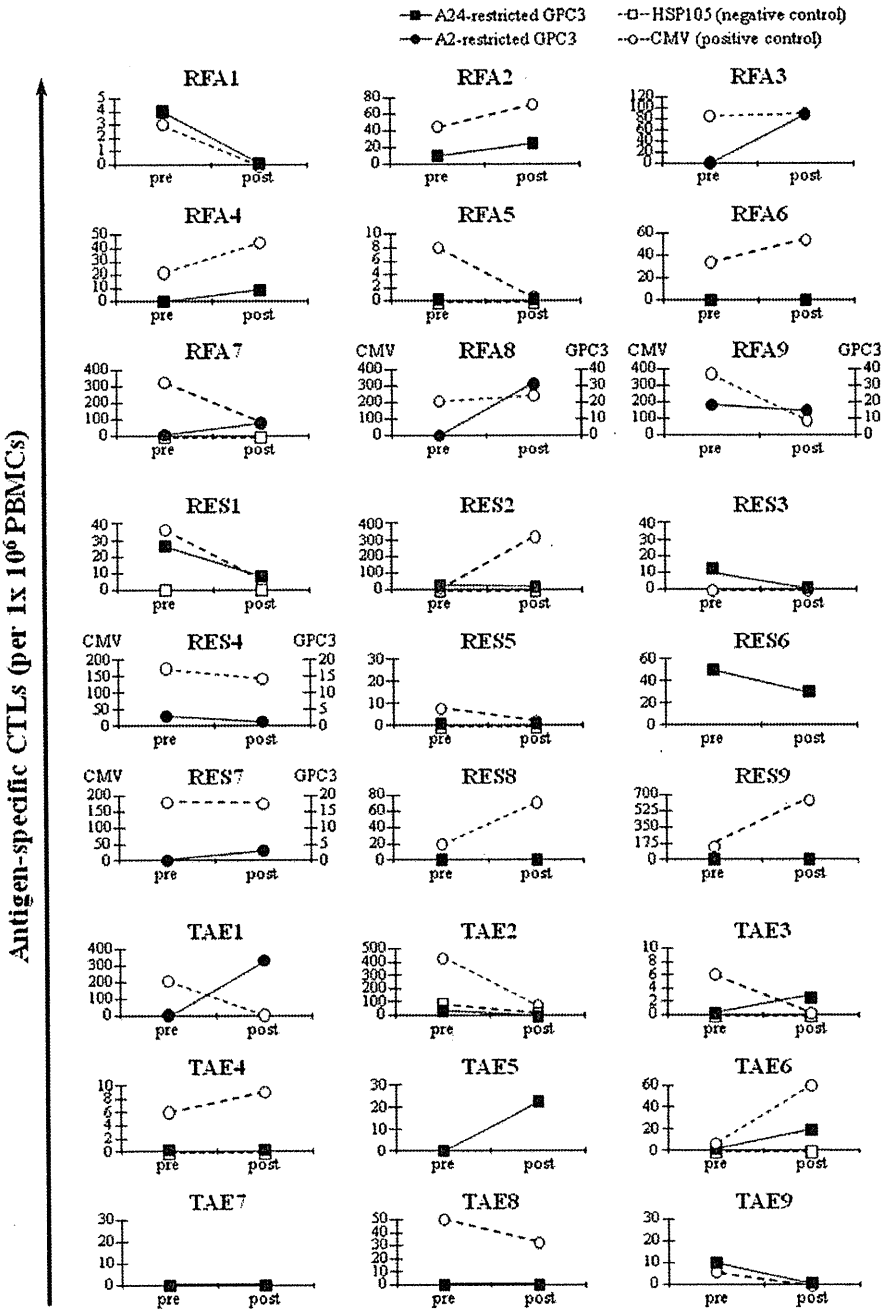

Figure 1. Kinetics of glypican-3 (GPC3)-specific CTLs between before and after treatment in each patient. A direct *ex vivo* interferon-γ enzyme-linked immunospot assay of PBMCs was performed before treatment and one month after treatment. The data are expressed as the number of interferon-γ producing cells, which indicate the CTLs specific with HLA-A24-restricted $GPC3_{298-306}$ peptide (EYILSLEEL) (■) or HLA-A2-restricted $GPC3_{144-152}$ peptide (FVGEFFTDV) (●). Heat shock protein 105 (HSP105) peptide (□) and cytomegalovirus (CMV) peptide (○) were used as the negative and positive control, respectively.

kinetics of tumor markers indicated that their treatment was effective. The frequency of GPC3-specific CTLs increased after RFA (RFA3) and TACE (TAE5), whereas it decreased after surgical resection (RES6).

RFA has the potential to strongly induce T-cell-mediated immune response: A case report. A 70-year-old woman was admitted because of recurrent HCCs. Thirteen months earlier, the patient had undergone RFA for primary HCC located in the S5/8 region of the liver. CT detected two recurrent HCCs: one was contiguous to the previously ablated S5/8 region and the other was a distant tumor located in the S6 region. We performed surgical resection for these recurrent HCCs. Immunohistochemical examination of CD8 in the resected tumors revealed that a marked number of $CD8^+$ T cells had infiltrated not only into the surrounding recurrent tumor but also into the distant recurrent tumor after RFA (Fig. 3). On the other hand, few $CD4^+$ T cells were observed in these tumors (data not shown). Immunohistochemical analyses showed the expression of GPC3 and HLA class I in these tumors (data not

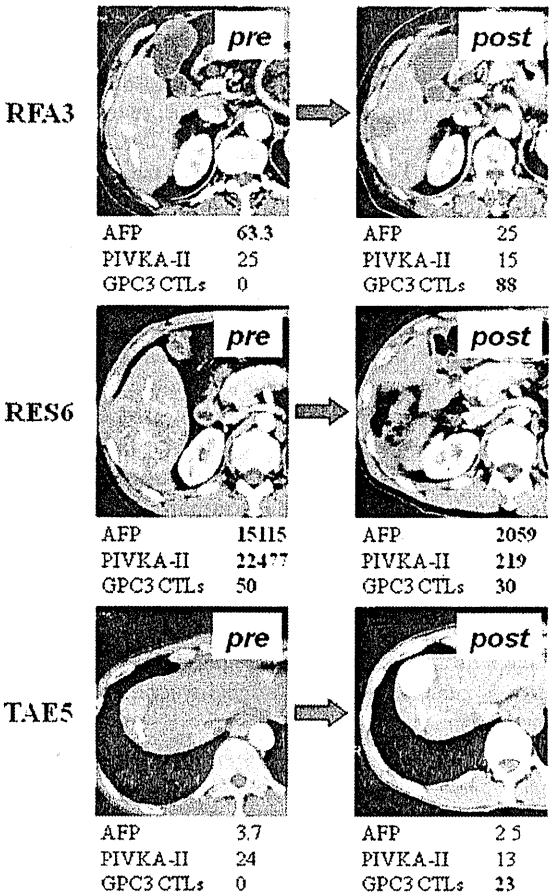

Figure 2. Changes in computed tomography images, serum levels of tumor markers, including α-fetoprotein (AFP) and protein induced by vitamin K absence or antagonist II (PIVKA-II), and glypican-3 (GPC3)-specific CTLs in PBMCs between before and after treatment in patients RFA3, RES6, and TAE5. White arrows indicate nodules of hepatocellular carcinoma at pre- and post-treatment. The bold letters show the abnormal levels of tumor markers or the positive response of GPC3 specific CTLs.

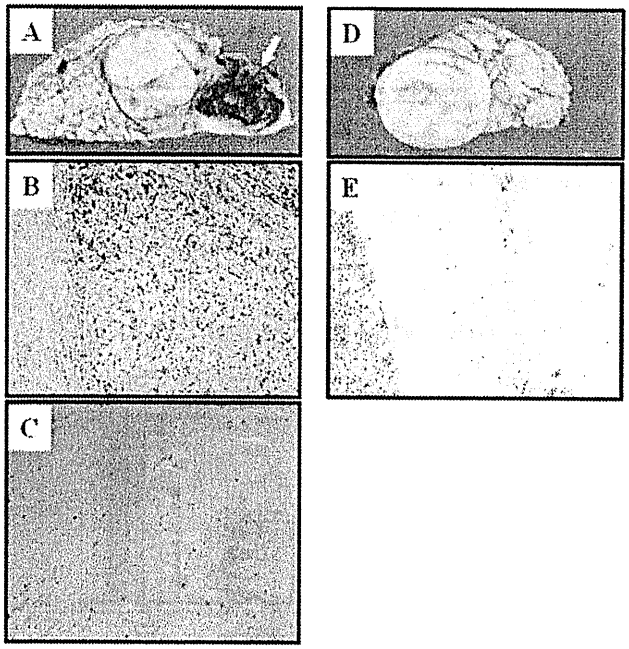

Figure 3. Macroscopic features and immunohistochemical examination of $CD8^+$ T cells in the resected tumors that had recurred after radiofrequency ablation. (A and D) show the cut surface of the resected specimens. (A) The white arrow indicates the post-ablated lesion to which a recurrent tumor was contiguous. The other recurrent tumor was distant from the post-ablated lesion (D). A marked number of $CD8^+$ T cells had infiltrated into the contiguous recurrent tumor (B) and the distant recurrent tumor (E), whereas few $CD8^+$ T cells had infiltrated into the post-ablated necrotic lesion (C). Magnification x100 (B and C) and x40 (E).

shown). These findings suggest that RFA not only activates the immune response systemically but also induces local infiltration of CTLs into the tumors.

Analysis of immune response induced by RFA in a mouse model. The experimental schedule is shown in Fig. 4A. The IFN-γ ELISPOT assay with $CD8^+$ T cells from the lymph nodes of mice demonstrated that the number of spots against both Colon 26 (P=0.049) and Colon 26/GPC3 (P=0.049) was larger after RFA compared to without treatment. On the other hand, the number of spots did not increase after surgical resection. These results suggest that RFA induced a significantly larger number of both Colon 26- and Colon 26/GPC3-reactive CTLs compared to no treatment or surgical resection (Fig. 4B).

The difference in number of spots between Colon 26 and Colon 26/GPC3 in each mouse, which represents GPC3-specific CTLs, is shown in Fig. 4C. As an effect of prior peptide vaccination, GPC3-specific CTLs were detected in the no treatment group. The frequency of GPC3-specific CTLs increased after RFA and decreased after surgical resection. As a result, the frequency of GPC3-specific CTLs after RFA was significantly greater than that after surgical resection (P=0.049). These results suggest that RFA induced a significantly larger number of GPC3-specific CTLs compared to surgical resection (Fig. 4C).

Discussion

We previously reported that 39% of HCC patients had detectable GPC3-specific CTLs by a direct *ex vivo* IFN-γ ELISPOT assay (25). In this study, GPC3-specific CTLs were detectable before treatment in 11 of 27 patients (41%). Additionally, when we analyzed the patients with a prior treatment for HCCs using the same methods, 11 of 21 (52%) patients had detectable GPC3-specific CTLs (data not shown). These results are favorable for anticancer immunotherapy because the antigen-specific T-cell-mediated immune response could be detected without *in vitro* stimulation. As for frequency, GPC3-specific CTLs were detectable in ~40% of HCC patients, whereas AFP-, human telomerase reverse transcriptase (hTERT)-, and multidrug resistance-associated protein 3 (MRP3)-specific CTLs have been detected in 5-20, 6-12, and 14-21% of HCC patients with a single epitope peptide, respectively (26-28). As for tumor stages, a GPC3-specific immune response is frequently detected even in the early stages (24), whereas AFP-specific CTLs are more frequently detected in patients with advanced HCC (26). These results suggest that GPC3 has strong immunogenicity and GPC3-specific T-cell-mediated immunotherapy is suitable for adjuvant therapy against HCC because the induction of tumor-specific immune response in

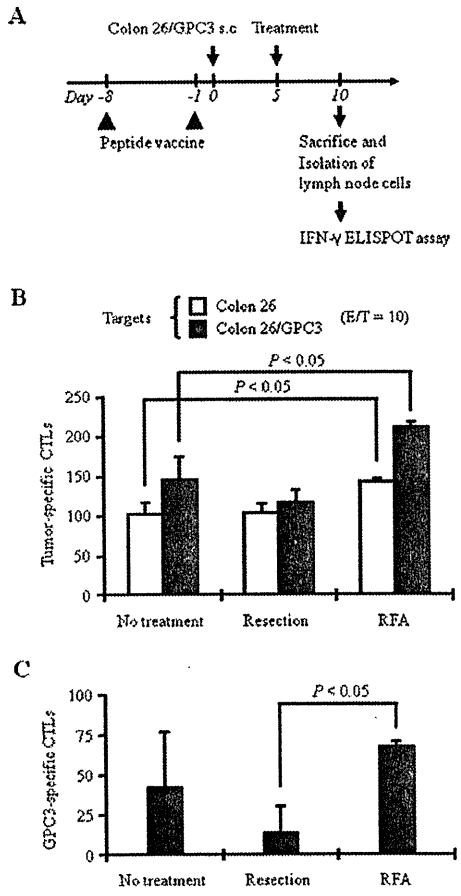

Figure 4. Investigation of the glypican-3 (GPC3)-specific immune response in a mouse model. (A) Experiment schedule. (B) An *ex vivo* interferon (IFN)-γ enzyme-linked immunospot (ELISPOT) assay of $CD8^+$ lymph node cells (effector, $3x10^5$ cells/well) against Colon 26 and Colon 26/GPC3 (target, $3x10^4$ cells/well). No treatment column indicates the group of mice that received only the peptide vaccination and no therapy for the established tumor. The data are expressed as the mean + SD. Three mice were used for each group. Effector/target ratio=10. (C) The frequency of GPC3-specific CTLs, which is calculated from the difference in the number of spots between Colon 26 and Colon 26/GPC3 in each mouse.

the early stages would be more effective for suppression of tumor growth.

The association between the induction of an antigen-specific immune response and the antigen expression in tumor tissue remains unclear. In this study, we obtained the result that the presence of GPC3-specific CTLs in PBMCs potentially had a positive correlation with GPC3 expression in tumor tissue, but the correlation was not statistically significant. On the other hand, Mizukoshi *et al* showed a negative correlation between the frequency of MRP3-specific CTLs and MRP3 expression level (28). Moreover, Benavides *et al* showed that even antigen-naïve patients had pre-existing immunity (29). First, this may be because of tumor heterogeneity of cancer tissue. In most cases, the whole tumor cannot be evaluated and, in the case of truly antigen-naïve patients, antigen-specific CTLs cannot exist in theory. Second, antigen expression may be negative if antigen-specific CTLs have killed all of the antigen-expressing tumor cells as described by Jäger *et al* (30). As for the changes in an antigen-specific immune response between before and after treatment, in this study, we showed impressive data that all patients with GPC3-expressing HCCs exhibited an increase in GPC3-specific CTLs after RFA or TACE, whereas no patient with GPC3-expressing HCCs did after surgical resection.

This is the first study to compare locoregional therapies, including RFA, surgical resection, and TACE, in terms of antigen-specific T-cell response in HCC patients and tumor-bearing mice. Half the patients after RFA or TACE showed an increase in GPC3-specific CTLs, which might have been induced by the treatment, whereas only 1 of 9 patients after resection showed an increase and more than half the patients after resection showed a decrease. Similarly, the frequency of GPC3-specific CTLs increased after RFA and decreased after resection in a mouse model. These results suggest that RFA induced a stronger GPC3-specific immune response compared to surgical resection. RFA destroys tumor tissue and causes local necrosis followed by the release of tumor-associated antigens (12), whereas all of the tumor-associated antigens must be completely removed after resection. With regard to TACE, whereas the results of an IFN-γ ELISPOT assay after TACE were as encouraging as that after RFA, we have no other favorable data on the immune response after TACE. Although further investigation is required, TACE, which is also a necrosis-inducing treatment, might induce an antigen-specific immune response.

A limitation of this study is the patient selection in the three kinds of locoregional therapy. Current treatment guidelines for HCC including the Japanese ones, which we followed in this study, recommend RFA to earlier HCCs and TACE to more advanced HCCs than those which receive surgical resection (2,31-33). Therefore, selection bias is unavoidable under the circumstances. To overcome this problem, we added a murine study. The advantage of RFA over surgical resection in the induction of GPC3-specific CTLs was demonstrated also in a mouse model.

The correlation between antitumor immune response and clinical response is controversial. In this study, a significant contribution of GPC3-specific CTLs toward an optimal prognosis was not demonstrated. Mizukoshi *et al* reported that enhancement of T-cell response did not last for long and did not contribute to the prevention of HCC recurrence (34). In view of the highly complex nature of the human immune system, patient prognoses might not be determined only by the CTL response. Previous studies have demonstrated that the release of tumor-derived antigens by necrosis-inducing treatment causes sufficient signaling to activate not only antigen-specific CTL response but also antigen-specific helper T-cell response (35,36), antigen-specific antibody response (36), and non-antigen-specific natural killer cell response (37). However, the mechanisms for cancer escape from immunosurveillance would suppress the efficiency of these immune responses (38). In the literature, tumor-infiltrating lymphocytes in HCC are associated with better prognosis (39), but, in our case, tumor-infiltrating CTLs were actually insufficient for suppression of cancer recurrence despite the massive infiltration. For successful anticancer immunotherapy, the development of an innovative strategy to link antitumor immune response with clinical response and to provide a survival benefit for cancer patients is necessary, and so we have just started the clinical trial of a GPC3-derived peptide vaccine for adjuvant therapy after RFA.

In conclusion, our results demonstrate that RFA has a stronger effect on the immune system compared with surgical resection. Although further investigation is necessary, the data on immune response support the rationale for combined immunotherapy for HCC patients.

Acknowledgements

D.N. would like to thank the Foundation for Promotion of Cancer Research (Japan) for the Third-Term Comprehensive Control Research for Cancer for awarding them a research resident fellowship. This study was supported in part by Health and Labor Science Research Grants for Research on Hepatitis from the Ministry of Health, Labor, and Welfare, Japan. J.F. received honoraria and consulting fee from Bayer, Chugai, Eisai, Eli Lilly, Taiho and Phizer; J.F.'s institute received grants from Pfizer and Bayer.

References

1. Parkin DM: Global cancer statistics in the year 2000. Lancet Oncol 2: 533-543, 2001.
2. Makuuchi M, Kokudo N, Arii S, *et al*: Development of evidence-based clinical guidelines for the diagnosis and treatment of hepatocellular carcinoma in Japan. Hepatol Res 38: 37-51, 2008.
3. Imamura H, Matsuyama Y, Tanaka E, *et al*: Risk factors contributing to early and late phase intrahepatic recurrence of hepatocellular carcinoma after hepatectomy. J Hepatol 38: 200-207, 2003.
4. Tateishi R, Shiina S, Yoshida H, *et al*: Prediction of recurrence of hepatocellular carcinoma after curative ablation using three tumor markers. Hepatology 44: 1518-1527, 2006.
5. Nobuoka D, Kato Y, Gotohda N, *et al*: Postoperative serum alpha-fetoprotein level is a useful predictor of recurrence after hepatectomy for hepatocellular carcinoma. Oncol Rep 24: 521-528, 2010.
6. Printz C: Clinical trials of note. Sorafenib as adjuvant treatment in the prevention of disease recurrence in patients with hepatocellular carcinoma (HCC) (STORM). Cancer 115: 4646, 2009.
7. Schwartz JD, Schwartz M, Mandeli J and Sung M: Neoadjuvant and adjuvant therapy for resectable hepatocellular carcinoma: review of the randomised clinical trials. Lancet Oncol 3: 593-603, 2002.
8. Ishii H, Yamamoto J and Ikari T: Adjuvant treatments for resectable hepatocellular carcinoma. J Hepatobiliary Pancreat Surg 15: 459-462, 2008.
9. Wissniowski TT, Hänsler J, Neureiter D, *et al*: Activation of tumor-specific T lymphocytes by radio-frequency ablation of the VX2 hepatoma in rabbits. Cancer Res 63: 6496-6500, 2003.
10. den Brok MH, Sutmuller RP, Nierkens S, *et al*: Efficient loading of dendritic cells following cryo and radiofrequency ablation in combination with immune modulation induces anti-tumour immunity. Br J Cancer 95: 896-905, 2006.
11. McGahan JP, Brock JM, Tesluk H, Gu WZ, Schneider P and Browning PD: Hepatic ablation with use of radio-frequency electrocautery in the animal model. J Vasc Interv Radiol 3: 291-297, 1992.
12. Yang WL, Nair DG, Makizumi R, *et al*: Heat shock protein 70 is induced in mouse human colon tumor xenografts after sublethal radiofrequency ablation. Ann Surg Oncol 11: 399-406, 2004.
13. Ali MY, Grimm CF, Ritter M, *et al*: Activation of dendritic cells by local ablation of hepatocellular carcinoma. J Hepatol 43: 817-822, 2005.
14. Filmus J: The contribution of in vivo manipulation of gene expression to the understanding of the function of glypicans. Glycoconj J 19: 319-323, 2002.
15. Nakatsura T, Yoshitake Y, Senju S, *et al*: Glypican-3, over-expressed specifically in human hepatocellular carcinoma, is a novel tumor marker. Biochem Biophys Res Commun 306: 16-25, 2003.
16. Nakatsura T and Nishimura Y: Usefulness of the novel oncofetal antigen glypican-3 for diagnosis of hepatocellular carcinoma and melanoma. BioDrugs 19: 71-77, 2005.
17. Shirakawa H, Kuronuma T, Nishimura Y, *et al*: Glypican-3 is a useful diagnostic marker for a component of hepatocellular carcinoma in human liver cancer. Int J Oncol 34: 649-656, 2009.
18. Nakatsura T, Komori H, Kubo T, *et al*: Mouse homologue of a novel human oncofetal antigen, glypican-3, evokes T-cell-mediated tumor rejection without autoimmune reactions in mice. Clin Cancer Res 10: 8630-8640, 2004.
19. Komori H, Nakatsura T, Senju S, *et al*: Identification of HLA-A2- or HLA-A24-restricted CTL epitopes possibly useful for glypican-3-specific immunotherapy of hepatocellular carcinoma. Clin Cancer Res 12: 2689-2697, 2006.
20. Motomura Y, Ikuta Y, Kuronuma T, *et al*: HLA-A2 and -A24-restricted glypican-3-derived peptide vaccine induces specific CTLs: preclinical study using mice. Int J Oncol 32: 985-990, 2008.
21. Shirakawa H, Suzuki H, Shimomura M, *et al*: Glypican-3 expression is correlated with poor prognosis in hepatocellular carcinoma. Cancer Sci 100: 1403-1407, 2009.
22. Yoshikawa T, Nakatsugawa M, Suzuki S, *et al*: HLA-A2-restricted glypican-3 peptide-specific CTL clones induced by peptide vaccine show high avidity and antigen-specific killing activity against tumor cells. Cancer Sci 102: 918-925, 2011.
23. Sobin LH and Wittekind C: UICC: TNM Classification of Malignant Tumors. 6th edition, Wiley-Liss, New York, pp81-83, 2002.
24. Tanaka Y, Eda H, Tanaka T, *et al*: Experimental cancer cachexia induced by transplantable colon 26 adenocarcinoma in mice. Cancer Res 50: 2290-2295, 1990.
25. Hayashi E, Motomura Y, Shirakawa H, *et al*: Detection of glypican-3-specific CTLs in chronic hepatitis and liver cirrhosis. Oncol Rep 22: 149-154, 2009.
26. Mizukoshi E, Nakamoto Y, Tsuji H, Yamashita T and Kaneko S: Identification of alpha-fetoprotein-derived peptides recognized by cytotoxic T lymphocytes in HLA-A24$^+$ patients with hepatocellular carcinoma. Int J Cancer 118: 1194-1204, 2006.
27. Mizukoshi E, Nakamoto Y, Marukawa Y, *et al*: Cytotoxic T cell responses to human telomerase reverse transcriptase in patients with hepatocellular carcinoma. Hepatology 43: 1284-1294, 2006.
28. Mizukoshi E, Honda M, Arai K, Yamashita T, Nakamoto Y and Kaneko S: Expression of multidrug resistance-associated protein 3 and cytotoxic T cell responses in patients with hepatocellular carcinoma. J Hepatol 49: 946-954, 2008.
29. Benavides LC, Gates JD, Carmichael MG, *et al*: The impact of HER2/neu expression level on response to the E75 vaccine: from U.S. Military Cancer Institute Clinical Trials Group Study I-01 and I-02. Clin Cancer Res 15: 2895-2904, 2009.
30. Jäger E, Ringhoffer M, Karbach J, Arand M, Oesch F and Knuth A: Inverse relationship of melanocyte differentiation antigen expression in melanoma tissues and CD8$^+$ cytotoxic-T-cell responses: evidence for immunoselection of antigen-loss variants in vivo. Int J Cancer 66: 470-476, 1996.
31. Llovet JM, Burroughs A and Bruix J: Hepatocellular carcinoma. Lancet 362: 1907-1917, 2003.
32. Bruix J and Sherman M: Practice Guidelines Committee, American Association for the Study of Liver Diseases: Management of hepatocellular carcinoma. Hepatology 42: 1208-1236, 2005.
33. Omata M, Lesmana LA, Tateishi R, *et al*: Asian Pacific Association for the Study of the Liver consensus recommendations on hepatocellular carcinoma. Hepatol Int 4: 439-474, 2010.
34. Mizukoshi E, Nakamoto Y, Arai K, *et al*: Enhancement of tumor-specific T-cell responses by transcatheter arterial embolization with dendritic cell infusion for hepatocellular carcinoma. Int J Cancer 126: 2164-2174, 2010.
35. Ayaru L, Pereira SP, Alisa A, *et al*: Unmasking of alpha-fetoprotein-specific CD4(+) T cell responses in hepatocellular carcinoma patients undergoing embolization. J Immunol 178: 1914-1922, 2007.
36. Widenmeyer M, Shebzukhov Y, Haen SP, *et al*: Analysis of tumor antigen-specific T cells and antibodies in cancer patients treated with radiofrequency ablation. Int J Cancer 128: 2653-2662, 2011.
37. Zerbini A, Pilli M, Laccabue D, *et al*: Radiofrequency thermal ablation for hepatocellular carcinoma stimulates autologous NK-cell response. Gastroenterology 138: 1931-1942, 2010.
38. Zerbini A, Pilli M, Penna A, *et al*: Radiofrequency thermal ablation of hepatocellular carcinoma liver nodules can activate and enhance tumor-specific T-cell responses. Cancer Res 66: 1139-1146, 2006.
39. Wada Y, Nakashima O, Kutami R, Yamamoto O and Kojiro M: Clinicopathological study on hepatocellular carcinoma with lymphocytic infiltration. Hepatology 27: 407-414, 1998.

Published OnlineFirst February 16, 2011; DOI:10.1158/1078-0432.CCR-10-2066

Clinical Cancer Research

Cancer Therapy: Preclinical

Preclinical Evaluation of Telomerase-Specific Oncolytic Virotherapy for Human Bone and Soft Tissue Sarcomas

Tsuyoshi Sasaki[1], Hiroshi Tazawa[2,3], Jo Hasei[1], Toshiyuki Kunisada[1,4], Aki Yoshida[1], Yuuri Hashimoto[3], Shuya Yano[3], Ryosuke Yoshida[3], Futoshi Uno[2,3], Shunsuke Kagawa[2,3], Yuki Morimoto[1], Yasuo Urata[5], Toshifumi Ozaki[1], and Toshiyoshi Fujiwara[2,3]

Abstract

Purpose: Tumor-specific replication-selective oncolytic virotherapy is a promising antitumor therapy for induction of cell death in tumor cells but not of normal cells. We previously developed an oncolytic adenovirus, OBP-301, that kills human epithelial malignant cells in a telomerase-dependent manner. Recent evidence suggests that nonepithelial malignant cells, which have low telomerase activity, maintain telomere length through alternative lengthening of telomeres (ALT). However, it remains unclear whether OBP-301 is cytopathic for nonepithelial malignant cells. Here, we evaluated the antitumor effect of OBP-301 on human bone and soft tissue sarcoma cells.

Experimental Design: The cytopathic activity of OBP-301, coxsackie and adenovirus receptor (CAR) expression, and telomerase activity were examined in 10 bone (OST, U2OS, HOS, HuO9, MNNG/HOS, SaOS-2, NOS-2, NOS-10, NDCS-1, and OUMS-27) and in 4 soft tissue (CCS, NMS-2, SYO-1, and NMFH-1) sarcoma cell lines. OBP-301 antitumor effects were assessed using orthotopic tumor xenograft models. The fiber-modified OBP-301 (termed OBP-405) was used to confirm an antitumor effect on OBP-301–resistant sarcomas.

Results: OBP-301 was cytopathic for 12 sarcoma cell lines but not for the non–CAR-expressing OUMS-27 and NMFH-1 cells. Sensitivity to OBP-301 was dependent on CAR expression and not on telomerase activity. ALT-type sarcomas were also sensitive to OBP-301 because of upregulation of human telomerase reverse transcriptase (*hTERT*) mRNA following virus infection. Intratumoral injection of OBP-301 significantly suppressed the growth of OST and SYO-1 tumors. Furthermore, fiber-modified OBP-405 showed antitumor effects on OBP-301–resistant OUMS-27 and NMFH-1 cells.

Conclusions: A telomerase-specific oncolytic adenovirus is a promising antitumor reagent for the treatment of bone and soft tissue sarcomas. *Clin Cancer Res; 17(7); 1828–38. ©2011 AACR.*

Introduction

Bone and soft tissue sarcomas are annually diagnosed in 13,230 patients in the United States (1). They are the third most common cancer in children and account for 15.4% of all childhood malignancies. Treatment of patients with bone and soft tissue sarcomas requires a multidisciplinary approach that involves orthopedic oncologists, musculoskeletal radiologists and pathologists, radiation oncologists, medical and pediatric oncologists, and microvascular surgeons (2, 3). Despite major advances in the treatment of bone and soft tissue sarcomas, such as neoadjuvant and adjuvant multiagent chemotherapy and aggressive surgery, about one fourth of the patients show a poor response to conventional therapy, resulting in subsequent recurrence and leading to a poor prognosis (1). Therefore, the development of a novel therapeutic strategy is required to cure patients with bone and soft tissue sarcomas.

Recent advances in molecular biology have fostered remarkable insights into the molecular basis of neoplasia. More than 85% of all human cancers, but only a few normal somatic cells, show high telomerase activity (4–6). Telomerase activity has also been detected in 17% to 81% of bone and soft tissue sarcomas (7–10). Telomerase activation is considered to be a critical step in cancer development, and its activity is closely correlated with the expression of human telomerase reverse transcriptase

Authors' Affiliations: [1]Department of Orthopaedic Surgery, Okayama University Graduate School of Medicine, Dentistry and Pharmaceutical Sciences; [2]Center for Gene and Cell Therapy, Okayama University Hospital; Departments of [3]Gastroenterological Surgery and [4]Medical Materials for Musculoskeletal Reconstruction, Okayama University Graduate School of Medicine, Dentistry and Pharmaceutical Sciences, Okayama; and [5]Oncolys BioPharma, Inc., Tokyo, Japan

Note: Supplementary data for this article are available at Clinical Cancer Research Online (http://clincancerres.aacrjournals.org/).

Corresponding Author: Toshiyoshi Fujiwara, Department of Gastroenterological Surgery, Okayama University Graduate School of Medicine, Dentistry and Pharmaceutical Sciences, 2-5-1 Shikata-cho, Kita-ku, Okayama 700-8558, Japan. Phone: 81-86-235-7257; Fax: 81-86-221-8775. E-mail: toshi_f@md.okayama-u.ac.jp

doi: 10.1158/1078-0432.CCR-10-2066

Published OnlineFirst February 16, 2011; DOI:10.1158/1078-0432.CCR-10-2066

Translational Relevance

Bone and soft tissue sarcomas frequently occur in young children and show aggressive progression, resistance to conventional chemotherapy, and poor prognosis, indicating a requirement for novel antitumor therapy to improve the clinical outcome. Telomerase-specific replication-selective oncolytic virotherapy is emerging as a promising antitumor therapy. We developed an oncolytic adenovirus, OBP-301, that efficiently kills human epithelial malignant cells in a telomerase-dependent manner. However, alternative lengthening of telomeres (ALT)-type nonepithelial malignant cells show low telomerase activity, suggesting lower effectiveness of OBP-301 in these cells. Here, we showed that OBP-301 has antitumor effects on both non–ALT-type and ALT-type sarcoma cells through upregulation of human telomerase reverse transcriptase mRNA. Furthermore, coxsackie and adenovirus receptor–negative sarcoma cells were efficiently killed by fiber-modified OBP-301 (termed OBP-405) through virus–integrin binding. Thus, a telomerase-specific oncolytic adenovirus would greatly improve the clinical outcome of young patients with advanced sarcomas.

(*hTERT*; ref. 11). Recently, telomerase-specific replication-selective oncolytic virotherapy has emerged as a promising antitumor therapy for induction of tumor-specific cell death. We previously developed an oncolytic adenovirus, OBP-301, in which the *hTERT* promoter drives the expression of the *E1A* and *E1B* genes linked to an internal ribosome entry site (IRES; ref. 12). We determined that OBP-301 efficiently induced the selective killing of a variety of human malignant epithelial cells, such as colorectal, prostate, and non–small cell lung cancers, but not of normal cells (12, 13). Furthermore, a phase I clinical trial of OBP-301, which was conducted in the United States on patients with advanced solid tumors, indicated that OBP-301 is well tolerated by patients (14).

There are 2 known telomere-maintenance mechanisms in human malignant tumors (15, 16): telomerase activation (4–6) and telomerase-independent alternative lengthening of telomeres (ALT; ref. 17–19). The ALT-type mechanism is more prevalent in tumors arising from nonepithelial tissues than in those of epithelial origin (20, 21). Therefore, ALT-type nonepithelial malignant cells frequently show low telomerase activity, suggesting that they have a low sensitivity to OBP-301, which kills cancer cells in a telomerase-dependent manner. However, it remains to be determined whether OBP-301 can exert an antitumor effect on human nonepithelial and on epithelial malignancies.

Adenovirus infection is mainly mediated by interaction of the virus with the coxsackie and adenovirus receptor (CAR) expressed on host cells (22). Therefore, while CAR-expressing tumor cells are the main targets for oncolytic adenoviruses, tumor cells that lack CAR can escape from being killed by oncolytic adenoviruses. It has been reported that CAR is frequently expressed in human cancers of various organs such as the brain (23), thyroid (24), esophagus (25), gastrointestinal tract (26), and ovary (27). Bone and soft tissue sarcomas also express CAR (28–30). However, some populations of tumor cells lack CAR expression, suggesting a requirement for the development of a novel antitumor therapy against CAR-negative tumor cells. We recently developed fiber-modified OBP-301 (termed OBP-405), which can bind to not only CAR but also integrin molecules ($\alpha v\beta 3$ and $\alpha v\beta 5$) and efficiently kill CAR-negative tumor cells (31).

In the present study, we first investigated the *in vitro* cytopathic efficacy of OBP-301 against 14 human bone and soft tissue sarcoma cells. Next, the relationship between the cytopathic activity of OBP-301, CAR expression, and telomerase activity in human sarcoma cells was assessed. The *in vivo* antitumor effect of OBP-301 was also confirmed using orthotopic animal models. Finally, the antitumor effect of OBP-405 against OBP-301–resistant sarcoma cells was evaluated *in vitro* and *in vivo*.

Materials and Methods

Cell lines

The human osteosarcoma (HuO9; ref. 32), chondrosarcoma (OUMS-27; ref. 33), and synovial sarcoma (SYO-1; ref. 34) cell lines were previously established in our laboratory. The human osteosarcoma cell lines OST, HOS, and SaOS-2 were kindly provided by Dr. Satoru Kyo (Kanazawa University, Ishikawa, Japan). The human clear cell sarcoma cell line CCS was maintained in our laboratory. These cells were propagated as monolayer cultures in Dulbecco's modified Eagle's medium (DMEM). The human osteosarcoma cell line U2OS was obtained from the American Type Culture Collection (ATCC) and was grown in McCoy's 5a medium. The human osteosarcoma cell line MNNG/HOS was purchased from DS Pharma Biomedical and was maintained in Eagle's minimum essential medium containing 1% nonessential amino acids. The human osteosarcoma cell lines NOS-2 and NOS-10 (35), the human dedifferentiated chondrosarcoma cell line NDCS-1 (36), the human malignant peripheral nerve sheath cell line NMS-2 (37), and the human malignant fibrous histiocytoma cell line NMFH-1 (38) were kindly provided by Dr. Hiroyuki Kawashima (Niigata University, Niigata, Japan) and were grown in RPMI-1640 medium. The transformed embryonic kidney cell line 293 was obtained from the ATCC and maintained in DMEM. All media were supplemented with 10% heat-inactivated FBS, 100 units/mL penicillin, and 100 μg/mL streptomycin. The cells were maintained at 37°C in a humidified atmosphere with 5% CO_2.

Recombinant adenoviruses

The recombinant tumor-specific, replication-selective adenovirus OBP-301 (Telomelysin), in which the promoter

Published OnlineFirst February 16, 2011; DOI:10.1158/1078-0432.CCR-10-2066

element of the *hTERT* gene drives the expression of *E1A* and *E1B* genes linked with an IRES, was previously constructed and characterized (12, 13). OBP-405 is a telomerase-specific replication-competent adenovirus variant that was previously generated to express the RGD peptide in the fiber knob of OBP-301 (31). The *E1A*-deleted adenovirus vector dl312 and wild-type adenovirus serotype 5 (Ad5) were used as the control vectors. Recombinant viruses were purified by ultracentrifugation using cesium chloride step gradients, and their titers were determined by a plaque-forming assay by using 293 cells and they were stored at −80°C.

Cell viability assay

Cells were seeded on 96-well plates at a density of 1×10^3 cells/well 20 hours before viral infection. All cell lines were infected with OBP-301 or OBP-405 at multiplicity of infections (MOI) of 0, 0.1, 1, 10, 50, or 100 plaque forming units (PFU)/cell. Cell viability was determined on days 1, 2, 3, and 5 after virus infection, using a Cell Proliferation kit II (Roche Molecular Biochemicals) that was based on an XTT, sodium 3′-[1-(phenylaminocarbonyl)-3,4-tetrazolium]-bis (4-methoxy-6-nitro)benzene sulfonic acid hydrate, assay, according to the manufacturer's protocol. The ID_{50} value of OBP-301 for each cell line was calculated using cell viability data obtained on day 5 after virus infection.

Flow cytometric analysis

The cells (5×10^5) were labeled with mouse monoclonal anti-CAR (RmcB; Upstate Biotechnology), anti-human integrin αvβ3 (LM609; Chemicon International), or anti-human integrin αvβ5 (P1F6; Chemicon International) antibody for 30 minutes at 4°C. The cells were then incubated with fluorescein isothiocyanate (FITC)-conjugated rabbit anti-mouse IgG second antibody (Zymed Laboratories) and were analyzed using flow cytometry (FACS Array; Becton Dickinson). The mean fluorescence intensity (MFI) of CAR and integrin αvβ3 or αvβ5 for each cell line was determined by calculating the difference between the MFI in antibody-treated and nontreated cells from 3 independent experiments.

Quantitative real-time PCR analysis

U2OS cells, seeded on 6-well plates at a density of 5×10^5 cells/well 20 hours before viral infection, were infected with Ad5, OBP-301, or dl312 at an MOI of 10 or 100 PFUs/cell. Mock-infected cells were used as controls. Furthermore, to confirm the modulation of *hTERT* mRNA expression by OBP-301 infection, CAR-positive and *hTERT* mRNA-expressing human sarcoma cell lines were seeded on 6-well plates at a density of 5×10^4 cells/well 20 hours before viral infection and were infected with OBP-301 at an MOI of 100 PFUs/cell. Total RNA was extracted from the cells 2 days after virus infection by using the RNA-Bee reagent (Tel-Test Inc.). After synthesis of cDNA from 100 ng of total RNA, the levels of *hTERT* and glyceraldehyde-3-phosphate dehydrogenase (*GAPDH*) mRNA expression were determined using quantitative real-time PCR and a Step One Plus Real Time PCR System (Applied Biosystems) and TaqMan Gene Expression Assays (Applied Biosystems). The relative levels of *hTERT* mRNA expression were calculated by using the $2^{-\Delta\Delta Ct}$ method (39) after normalization with reference to the expression of *GAPDH* mRNA.

To compare the *E1A* copy number between OBP-301- and Ad5-infected U2OS cells, U2OS cells, seeded on 6-well plates at a density of 5×10^5 cells/well 20 hours before viral infection, were infected with OBP-301 or Ad5 at an MOI of 10 PFUs/cell. Genomic DNA was extracted from serially diluted viral stocks, and tumor cells were infected with OBP-301 or Ad5 by using the QIAmp DNA Mini Kit (Qiagen). *E1A* copy number was also determined using TaqMan real-time PCR systems (Applied Biosystems).

In vivo OST and OUMS-27 xenograft tumor models

Animal experimental protocols were approved by the Ethics Review Committee for Animal Experimentation of Okayama University School of Medicine. The OST and OUMS-27 cells (5×10^6 cells per site) were inoculated into the tibia or the flank of female athymic nude mice aged 6 to 7 weeks (Charles River Laboratories). Palpable tumors developed within 14 to 21 days and were permitted to grow to approximately 5 to 6 mm in diameter. At that stage, a 50 μL volume of solution containing OBP-301, OBP-405, dl312, or PBS was injected into the tumors. Tumor size was monitored by measuring tumor length and width by using calipers. The volumes of OUMS-27 tumors were calculated using the following formula: $(L \times W^2) \times 0.5$, where L is the length and W is the width of each tumor. The volumes of OST tumors were calculated using the formula: $(L + W) \times L \times W \times 0.2618$, as previously reported (40).

X-ray examination

The formation of osteolytic lesions was monitored using radiography (FUJIFILM IXFR film; FUJIFILM Co.) and an X-ray system (SOFTEX TYPE CMB; SOFTEX Co.).

Histopathologic analysis

Tumors were fixed in 10% neutralized formalin and embedded in paraffin blocks. Sections were stained with hematoxylin/eosin (H&E) and analyzed by light microscopy.

Statistical analysis

Data are expressed as means ± SD. Student's t test was used to compare differences between groups. Pearson's product–moment correlation coefficients were calculated using PASW statistics version 18 software (SPSS Inc.). Statistical significance was defined when the P value was less than 0.05.

Results

In vitro cytopathic efficacy of OBP-301 against human bone and soft tissue sarcoma cell lines

To evaluate the *in vitro* cytopathic effect of OBP-301 against nonepithelial malignant cells, 14 tumor cell lines

Published OnlineFirst February 16, 2011; DOI:10.1158/1078-0432.CCR-10-2066

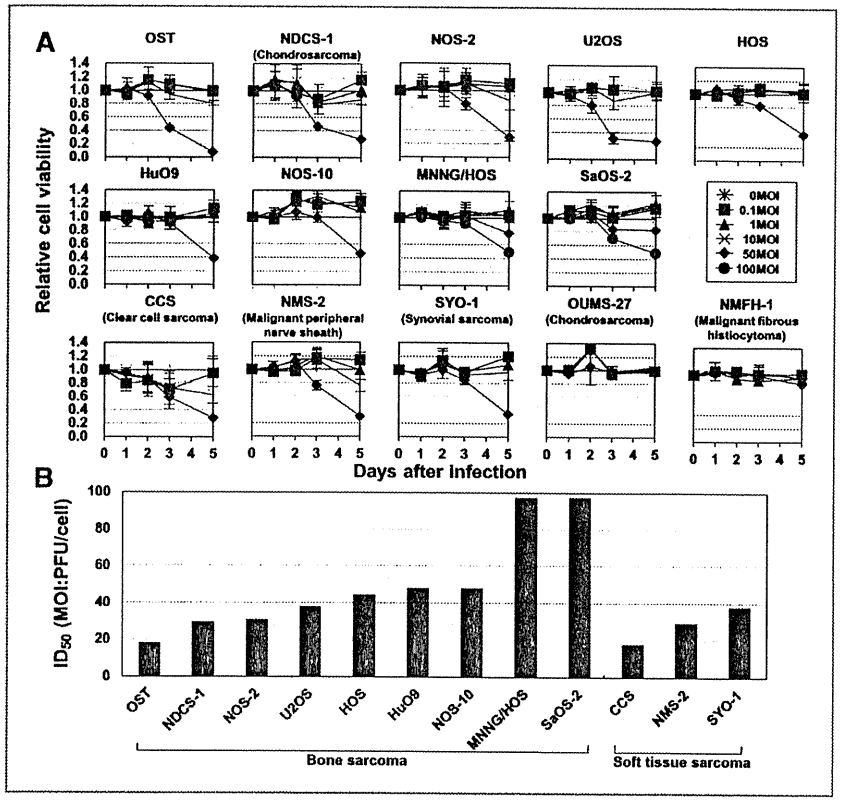

Figure 1. Cytopathic effect of OBP-301 on human bone and soft tissue sarcoma cell lines. A, cells were infected with OBP-301 at the indicated MOI, and cell survival was quantified over 5 days using the XTT assay. The cell viability of mock-treated group on each day was considered 1.0, and the relative cell viability was calculated. Data are means ± SD. The types of tumor except for osteosarcoma were shown in parentheses. B, the 50% inhibiting doses of OBP-301 on cell viability 5 days after infection were calculated and are expressed as ID_{50} values.

derived from human bone and soft tissue sarcomas were infected with various doses of OBP-301. The cell viability of each cell line was assessed over 5 days after infection by the XTT assay. OBP-301 infection induced cell death in a time-dependent manner in all sarcoma cell lines except for the OUMS-27 and NMFH-1 cell lines (Fig. 1A). Calculation of the ID_{50} values revealed that, of the 12 OBP-301–sensitive sarcoma cell lines, MNNG/HOS and SaOS-2 cells were relatively less sensitive than the other 10 sarcoma cell lines (Fig. 1B). Furthermore, to rule out the possibility that cytopathic effect of OBP-301 is due to nonspecific toxicity based on the high uptake of virus particles into tumor cells, we examined the cytopathic activity of replication-deficient dl312 in U2OS and HOS cells. dl312 did not show any cytopathic effect in U2OS and HOS cells, even when these cells were infected with dl312 at high dose (50 and 100 MOIs; Supplementary Fig. S1). These results indicate that OBP-301 is cytopathic for most human bone and soft tissue sarcoma cells line but that some sarcoma cell lines are resistant to OBP-301.

Expressions of the adenovirus receptor and *hTERT* mRNA on human bone and soft tissue sarcoma cell lines

Because adenovirus infection efficiency depends mainly on cellular CAR expression (22), we determined the expression level of CAR on the 14 sarcoma cell lines by flow cytometry. The 12 OBP-301–sensitive sarcoma cell lines showed CAR expression, determined as MFIs, at various levels, whereas the OBP-301–resistant OUMS-27 and NMFH-1 cells did not express CAR (Fig. 2A and Supplementary Fig. S2).

OBP-301 contains the *hTERT* gene promoter, which allows it to tumor specifically regulate the gene expression of *E1A* and *E1B* for viral replication. Thus, OBP-301 can efficiently replicate in human cancer cells with high telomerase activity but not in normal cells without telomerase activity (12). Recently, some populations of human sarcoma cells have been shown to possess low telomerase activity and to maintain telomere lengths through an ALT mechanism (17–19). Thus, it is probable that OBP-301 cannot efficiently replicate in, and kill, ALT-type human sarcoma cells because of their low telomerase activity. To assess whether the telomerase activity of human sarcoma cells affects the cytopathic activity of OBP-301, we analyzed *hTERT* mRNA expression levels in the 14 sarcoma cell lines by quantitative real-time reverse transcriptase PCR (RT-PCR) analysis. Thirteen of the sarcoma cell lines had detectable *hTERT* mRNA expression at variable levels, and only SaOS-2 cells did not express *hTERT* mRNA (Fig. 2B).

Published OnlineFirst February 16, 2011; DOI:10.1158/1078-0432.CCR-10-2066

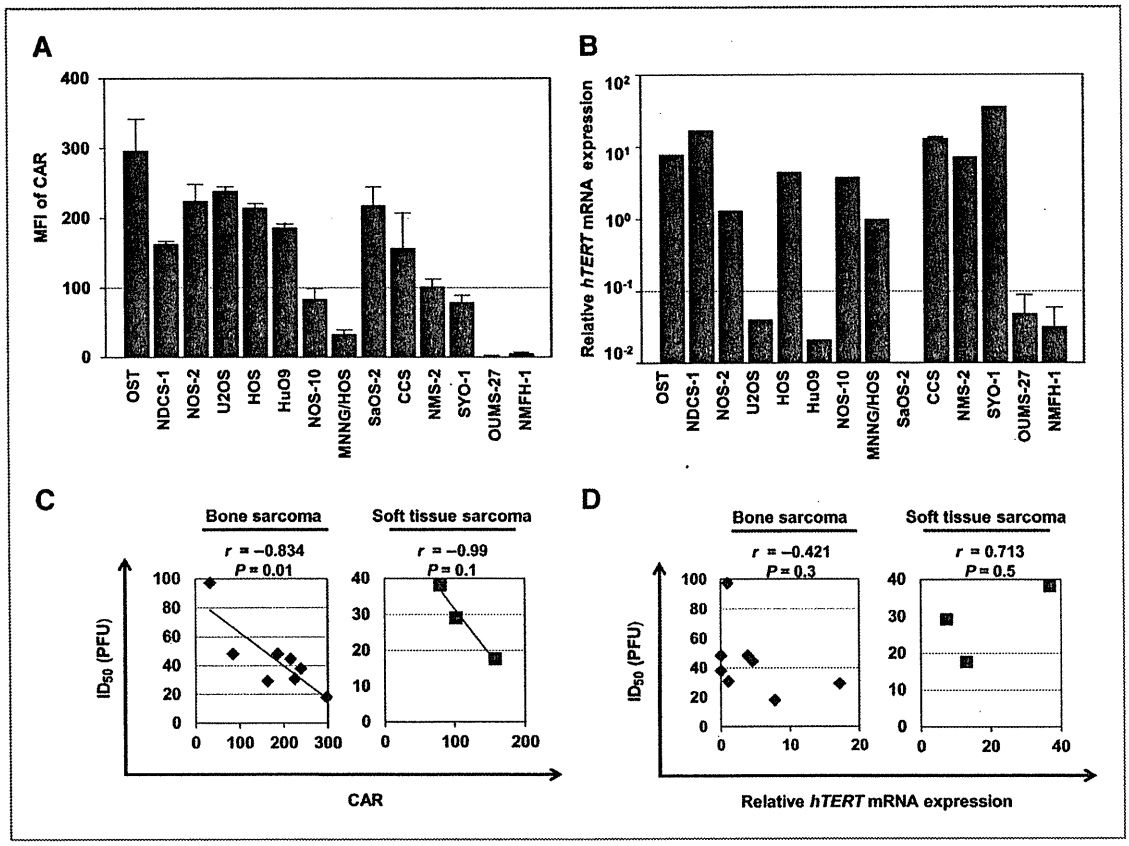

Figure 2. Relationship between the expression levels of CAR and *hTERT* mRNA and the cytopathic activity of OBP-301 against human bone and soft tissue sarcoma cell lines. A, the MFI of CAR expression on human bone and soft tissue sarcoma cells. The cells were incubated with a monoclonal anti-CAR (RmcB) antibody, followed by flow cytometric detection using an FITC-labeled secondary antibody. B, expression of *hTERT* mRNA in human bone and soft tissue sarcoma cells by quantitative real-time PCR. The relative levels of *hTERT* mRNA were calculated after normalization with reference to the expression of *GAPDH* mRNA. C, correlation between the MFI of CAR and the ID_{50} of OBP-301 on human bone and soft tissue sarcoma cells. D, correlation between *hTERT* mRNA expression and the ID_{50} of OBP-301 on human bone and soft tissue sarcoma cells. Statistical significance was determined as $P < 0.05$, after analysis of Pearson's correlation coefficient.

We next investigated the relationship between CAR and *hTERT* mRNA expressions and the cytopathic activity of OBP-301 among the 11 CAR-positive sarcoma cell lines with *hTERT* gene expression. CAR expression levels significantly ($r = -0.834$; $P = 0.01$) correlated with the cytopathic activity of OBP-301 against 8 of the bone sarcoma cell lines (Fig. 2C). CAR expression in 3 of the soft tissue sarcoma cell lines also correlated ($r = -0.99$) with the cytopathic effect of OBP-301, but the differences did not reach significance ($P = 0.1$) because of the low number of cell lines assayed. In contrast, there was no significant correlation between *hTERT* mRNA expression and the cytopathic activity of OBP-301 (Fig. 2D). These results indicate that the cytopathic activity of OBP-301, at least in part, depends on CAR expression.

Furthermore, SaOS-2 and U2OS cells have already been shown to be ALT-type sarcoma cell lines with low telomerase activity (9, 17). Among these ALT-type sarcoma cells, U2OS cells showed a sensitivity to OBP-301 that was similar to that of non–ALT-type sarcoma cells such as HOS and NOS-10 (Fig. 1B). These results indicate that ALT-type human sarcoma cells are sensitive to OBP-301 and that a low telomerase activity does not detract from the cytopathic activity of OBP-301.

Enhanced virus replication and cytopathic activity of OBP-301 through *hTERT* mRNA upregulation in ALT-type sarcoma cell lines

The high sensitivity of ALT-type sarcoma cells to OBP-301 prompted us to hypothesize that OBP-301 may activate the *hTERT* gene promoter, thereby enhancing the viral replication rate and subsequently inducing cytopathic activity in ALT-type sarcoma cells. Furthermore, it has been previously shown that the adenoviral E1A

Published OnlineFirst February 16, 2011; DOI:10.1158/1078-0432.CCR-10-2066

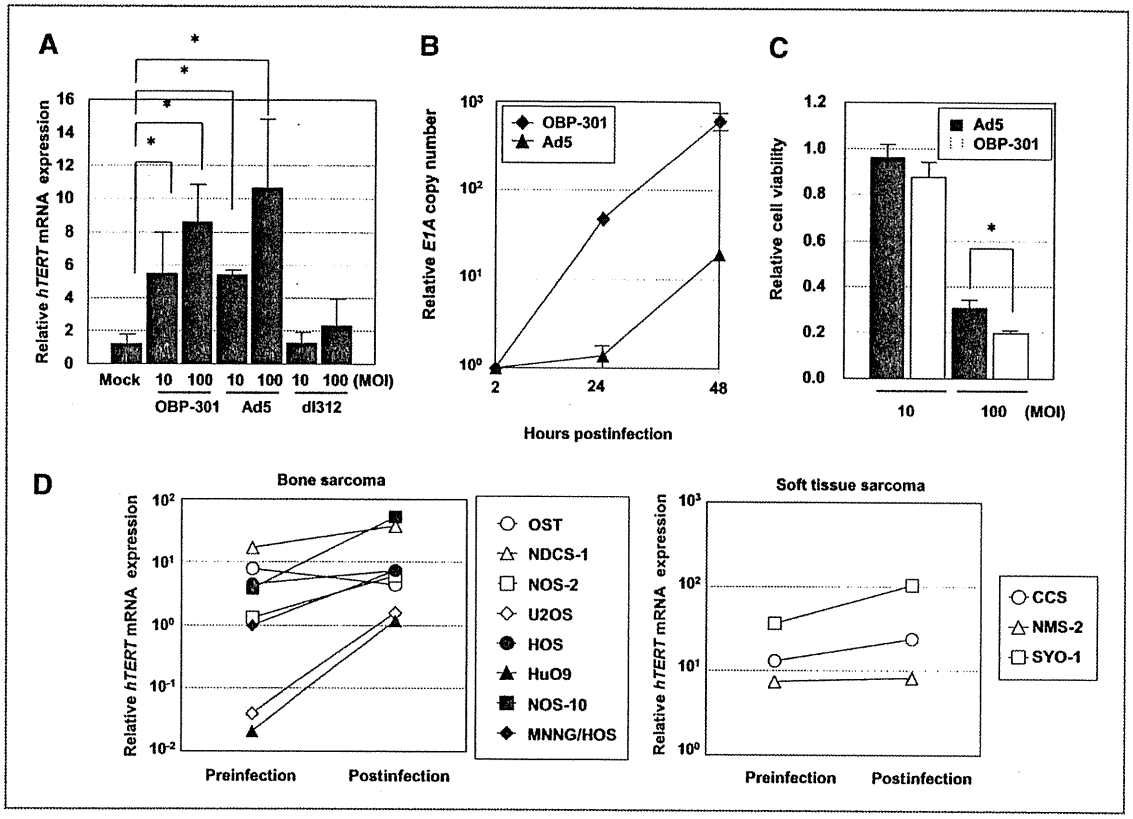

Figure 3. Upregulation of *hTERT* gene expression in ALT-type human sarcoma cell lines enhances the replication and the cytopathic effect of OBP-301. A, expression of *hTERT* mRNA in U2OS cells that were mock-infected or were infected with OBP-301, Ad5, or dl312. The cells were infected with OBP-301, Ad5, or dl312 at the indicated MOIs for 48 hour, and *hTERT* mRNA expression was analyzed using quantitative real-time RT-PCR. The value of *hTERT* mRNA expression in the mock-infected cells was set at 1, and relative mRNA levels were plotted. B, quantitative measurement of viral DNA replication in U2OS cells infected with OBP-301 or Ad5. The cells were infected with OBP-301 or Ad5 at an MOI of 10 PFUs/cell, and *E1A* copy number was analyzed over the following 2 days by quantitative real-time PCR. The value of the *E1A* copy number at 2 hours after infection was set at 1, and relative copy numbers were plotted. C, comparison of the cytopathic effect of OBP-301 and Ad5 in U2OS cells. The cells were infected with OBP-301 or Ad5 at the indicated MOIs, and cell survival was quantified 5 days after infection by using an XTT assay. D, expression of *hTERT* mRNA after infection of human bone (left) and soft tissue (right) sarcoma cell lines with OBP-301 at an MOI of 100 PFUs/cell. Statistical significance (*) was determined as $P < 0.05$ (Student's *t* test).

protein can activate the promoter activity of the *hTERT* gene (41, 42). Therefore, to determine whether OBP-301 infection activates *hTERT* mRNA expression, we examined the expression level of *hTERT* mRNA in ALT-type U2OS cells after infection with OBP-301 at MOIs of 10 and 100 PFUs/cell (Fig. 3A). Compared with mock-infected U2OS cells, OBP-301–infected U2OS cells showed a 6- to 8-fold increase in *hTERT* mRNA expression in a dose-dependent manner. Ad5 infection also increased *hTERT* mRNA expression in U2OS cells, whereas there was no increase in U2OS cells infected with *E1A*-deleted dl312. These results suggest that OBP-301 is cytopathic for ALT-type sarcoma cells through E1A-mediated activation of the *hTERT* gene promoter.

We next compared viral replication rates after infection of ALT-type U2OS cells with OBP-301 or Ad5. As expected, the viral replication rate of OBP-301 was significantly higher than that of Ad5 (Fig. 3B). Furthermore, the cytopathic activity of OBP-301 was significantly higher than that of Ad5 against the ALT-type U2OS cells (Fig. 3C). Finally, to determine whether OBP-301 activates *hTERT* mRNA expression in both ALT-type and non–ALT-type human sarcoma cell lines, we infected 11 CAR-positive human sarcoma cells with OBP-301 at 100 MOI. Ten of the 11 CAR-positive human sarcoma cell lines showed an increase in the expression level of *hTERT* mRNA after OBP-301 infection that ranged from a 1.1- to 50.0-fold increase (Fig. 3D and Supplementary Table S1). In addition, the expression level of *hTERT* mRNA was also upregulated when OST cells were infected with 5 or 50 MOI of OBP-301 (Supplementary Fig. S3). These results suggest that OBP-301 is cytopathic for both ALT-type and non–ALT-type human sarcoma cells through activation of the *hTERT* gene promoter.

Published OnlineFirst February 16, 2011; DOI:10.1158/1078-0432.CCR-10-2066

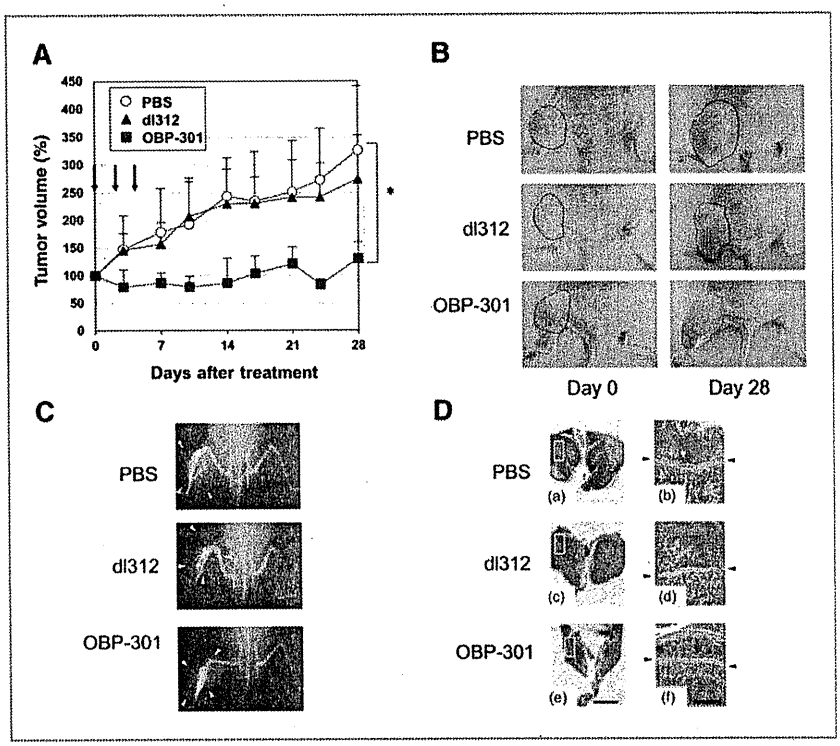

Figure 4. Antitumor effect of OBP-301 in an orthotopic OST bone sarcoma xenograft model. A, athymic nude mice were inoculated intratibially with OST cells (5×10^6 cells/site). Fourteen days after inoculation (designated as day 0), OBP-301 (■) or OBP-405 (▲) was injected into the tumor, with 1×10^8 PFUs on days 0, 2, and 4. PBS (○) was used as a control. Four mice were used for each group. Tumor growth was expressed as mean tumor volume ± SD. Statistical significance (*) was determined as $P < 0.05$ (Student's t test). B, macroscopic appearance of OST tumors in nude mice on days 0 and 28 after treatment with PBS, dl312, or OBP-301. Tumor masses are outlined by a dotted line. C, X-ray photographs of mice bearing OST tumors. The white arrowheads indicate the space occupied by the tumor mass. D, histologic analysis of the OST tumors. Tumor sections were obtained 28 days after inoculation of tumor cells. Paraffin-embedded sections of OST tumors were stained with H&E. The black arrowheads indicate growth plate cartilages. a, c and e, are low-magnification images and b, d and f are high-magnification images of the area outlined by a white square. Left scale bar, 5 mm. Right scale bar, 500 μm.

Antitumor effect of OBP-301 against 2 orthotopic tumor xenograft models

To evaluate the *in vivo* antitumor effect of OBP-301 against human bone and soft tissue sarcomas, we used 2 types of orthotopic tumor xenograft models: the OST bone sarcoma xenograft and the SYO-1 subcutaneous soft tissue sarcoma xenograft. We first identified a dose of OBP-301 that was suitable for induction of an antitumor effect in the subcutaneous OST bone sarcoma xenograft model (determined as $>10^7$ PFUs; Supplementary Fig. S4). We next assessed the antitumor effect of OBP-301 on the orthotopic OST bone sarcoma xenograft model. OBP-301 was injected into the tumor once a day for 3 days, with 10^8 PFUs per day (10). Replication-deficient adenovirus dl312 or PBS was also injected into control groups. Tumor growth was significantly suppressed by OBP-301 injection compared with injection of dl312 or PBS (Fig. 4A). Macroscopic analysis of the tumors indicated that OBP-301–treated tumors were consistently smaller than dl312- or PBS-treated tumors on day 28 after treatment (Fig 4B). We further determined whether OBP-301–treated tumors were less destructive to surrounding normal tissues than control tumors, using X-ray and histologic analyses (Fig. 4C and D). X-ray examination revealed that OBP-301–treated tumors resulted in less bone destruction than dl312- or PBS-treated tumors. Histologic findings were consistent with the X-ray results, showing that some tumor tissue had penetrated over the growth plate cartilage in dl312- and PBS-treated tumors but not in OBP-301–treated tumors.

With future clinical application in mind, we sought to establish a suitable protocol for repeated intratumoral injection of OBP-301 by using an orthotopic SYO-1 soft tissue sarcoma xenograft model. Doses of OBP-301 that were suitable for induction of an antitumor effect on SYO-1 tumors ($>10^8$ PFUs) were determined in a manner similar to that of OST bone sarcoma cells (data not shown). OBP-301 was injected 3 times into the tumor, with 10^9 PFUs and intervals of 1 day, 2 days, or 1 week between injections (Supplementary Fig. S5). A total of 3 OBP-301 injections, with intervals of 2 days or 1 week between injections, induced a significant

Published OnlineFirst February 16, 2011; DOI:10.1158/1078-0432.CCR-10-2066

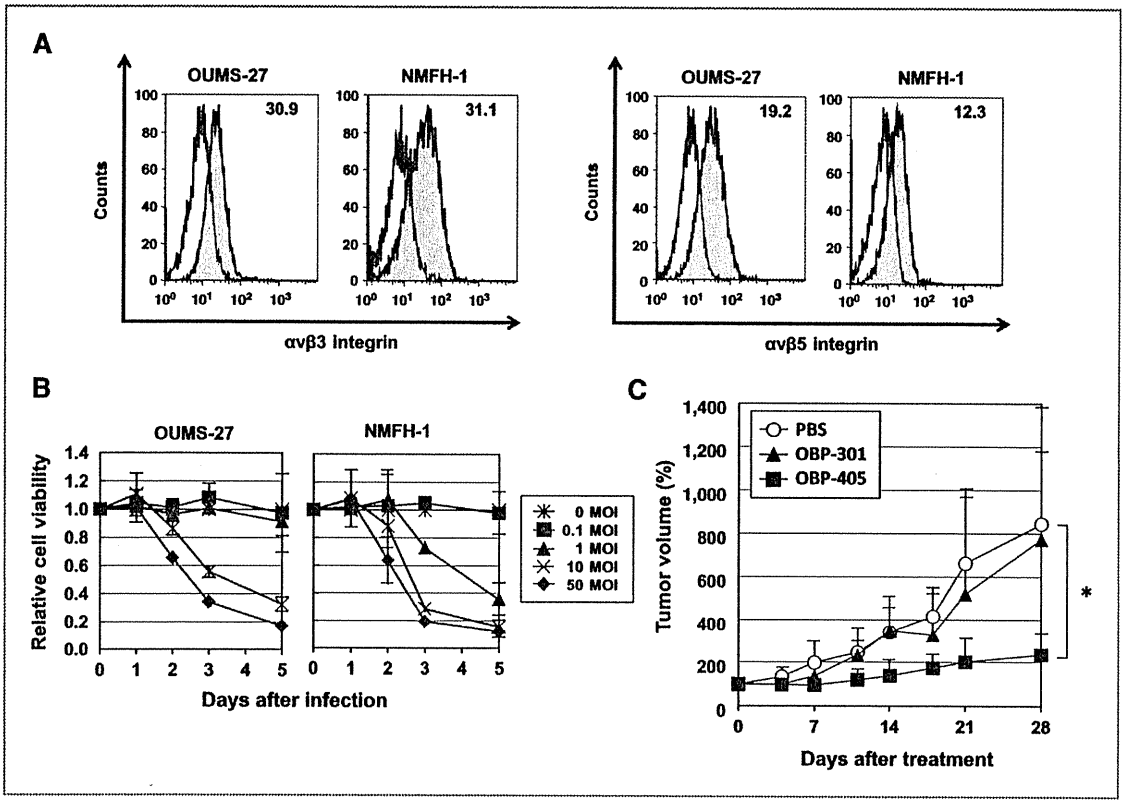

Figure 5. *In vitro* and *in vivo* antitumor effects of OBP-405 on OBP-301–resistant human sarcoma cell lines. A, expression of the integrins αvβ3 (left) and αvβ5 (right) on OUMS-27 and NMFH-1 cells. The cells were incubated with a monoclonal anti-αvβ3 integrin (LM609) or an anti-αvβ5 integrin (P1F6), followed by flow cytometric detection using an FITC-labeled secondary antibody. The gray histogram represents integrin antibody staining. The number at the top right-hand corner of each graph is the MFI. B, cytopathic effect of OBP-405 on OUMS-27 and NMFH-1 cells. The cells were infected with OBP-405 at the indicated MOI values, and cell survival over 5 days was quantified using an XTT assay. C, antitumor effect of OBP-405 in a subcutaneous OUMS-27 xenograft tumor model. Athymic nude mice were inoculated subcutaneously with OUMS-27 cells (5×10^6 cells/site). Fourteen days after inoculation (designated as day 0), OBP-301 (▲) or OBP-405 (■) was injected into the tumor, with 1×10^8 PFUs on days 0, 2, and 4. PBS (○) was used as a control. Ten mice were used for each group. Tumor growth was expressed as the mean tumor volume ± SD. Statistical significance (*) was determined as $P < 0.05$ (Student's *t* test).

suppression of tumor growth, whereas intervals of 1 day between injections were not effective. These results suggest that an interval of more than 2 days between injections is necessary to efficiently suppress tumor growth by repeated injections of OBP-301.

Antitumor effect of OBP-405 on OBP-301–resistant sarcoma cell lines

OUMS-27 and NMFH-1 cells are resistant to OBP-301 because they lack CAR expression (Fig. 1A and Supplementary Fig. S2). We previously developed a fiber-modified OBP-301, termed OBP-405, which can enter not only CAR-positive cancer cells but also CAR-negative cancer cells through binding to the cell surface integrins αvβ3 and αvβ5 (31). We therefore sought to evaluate the antitumor effect of OBP-405 on the OBP-301–resistant OUMS-27 and NMFH-1 cells. We first examined the expression levels of the integrins αvβ3 and αvβ5 on the surface of these cells by flow cytometry (Fig. 5A). OUMS-27 and NMFH-1 cells expressed both integrin molecules. We next examined the effect of OBP-405 on OUMS-27 and NMFH-1 cell viability by using the XTT assay (Fig. 5B). OBP-405 efficiently suppressed cell viability of both of these cell lines in a dose- and time-dependent manner. We further assessed whether OBP-405 has an *in vivo* antitumor effect by assaying the effect of 3 intratumoral injections of OBP-301 or OBP-405, with 10^8 PFUs or of control PBS, into subcutaneous OUMS-27 tumor xenografts. As shown in Figure 5C, administration of OBP-405 resulted in significant suppression of tumor growth compared with OBP-301- or PBS-treated tumors 28 days after treatment. These results suggest that fiber-modified OBP-405 is a potential antitumor reagent that is effective against CAR-negative human sarcoma cells.